/

Article / Book Information

Title	Rigidity and soft percolation in the glass transition of an atomistic model of ionicliquid, 1-ethyl-3-methyl imidazolium nitrate, from molecular dynamics
Authors	JUNKO HABASAKI,Kia L. Ngai
Citation	J. Chem. Phys., 142, ,
Pub. date	2015, 4
URL	http://scitation.aip.org/content/aip/journal/jcp
Copyright	Copyright (c) 2015 American Institute of Physics

Rigidity and soft percolation in the glass transition of an atomistic model of ionic liquid, 1-ethyl-3-methyl imidazolium nitrate, from molecular dynamics simulations—Existence of infinite overlapping networks in a fragile ionic liquid

Junko Habasaki and K. L. Ngai

Articles you may be interested in

Designing heavy metal oxide glasses with threshold properties from network rigidity
J. Chem. Phys. **140**, 014503 (2014); 10.1063/1.4855695

Superstrong nature of covalently bonded glass-forming liquids at select compositions
J. Chem. Phys. **139**, 164511 (2013); 10.1063/1.4826463

Shear modulus of simulated glass-forming model systems: Effects of boundary condition, temperature, and sampling time
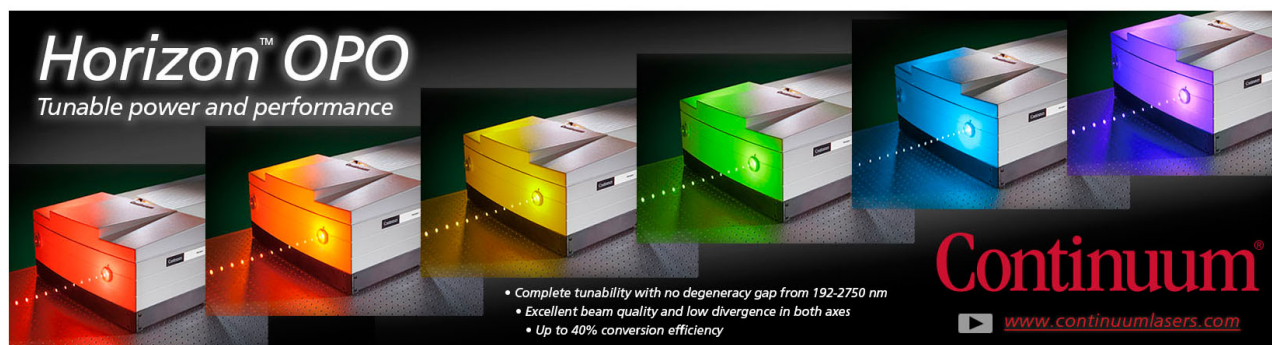J. Chem. Phys. **138**, 12A533 (2013); 10.1063/1.4790137

Atomistic simulations of the solid-liquid transition of 1-ethyl-3-methyl imidazolium bromide ionic liquid
J. Chem. Phys. **135**, 144501 (2011); 10.1063/1.3641486

Ionic diffusion and the topological origin of fragility in silicate glasses
J. Chem. Phys. **131**, 244514 (2009); 10.1063/1.3276285

Rigidity and soft percolation in the glass transition of an atomistic model of ionic liquid, 1-ethyl-3-methyl imidazolium nitrate, from molecular dynamics simulations—Existence of infinite overlapping networks in a fragile ionic liquid

Junko Habasaki[1,a)] and K. L. Ngai[2]

[1]*Department of Innovative and Engineered Materials, Interdisciplinary Graduate School of Science and Engineering, Tokyo Institute of Technology, Nagatsuta 4259, Yokohama 226-8502, Japan*
[2]*CNR-IPCF Dipartimento di Fisica, Università di Pisa, Largo Bruno Pontecorvo 3, I-56127 Pisa, Italy*

The typical ionic liquid, 1-ethyl-3-methyl imidazolium nitrate (EMIM-NO$_3$), was examined by molecular dynamics simulations of an all-atomistic model to show the characteristics of networks of cages and/or bonds in the course of vitrification of this fragile glass-former. The system shows changes of dynamics at two characteristic temperatures, T_B (or T_c) and the glass transition temperature T_g, found in other fragile glass forming liquids [K. L. Ngai and J. Habasaki, J. Chem. Phys. **141**, 114502 (2014)]. On decreasing temperature, the number of neighboring cation-anion pairs, N_B, within the first minimum of the pair correlation function, $g(r)_{min}$, increases. On crossing T_B ($>T_g$), the system volume and diffusion coefficient both show changes in temperature dependence, and as usual at T_g. The glass transition temperature, T_g, is characterized by the saturation of the total number of "bonds," N_B and the corresponding decrease in degree of freedom, $F = [(3N - 6) - N_B]$, of the system consisting of N particles. Similar behavior holds for the other ion-ion pairs. Therefore, as an alternative, the dynamics of glass transition can be interpreted conceptually by rigidity percolation. Before saturation occurring at T_g, the number of bonds shows a remarkable change at around T_B. This temperature is associated with the disappearance of the loosely packed coordination polyhedra of anions around cation (or vice versa), related to the loss of geometrical freedom of the polyhedra, f_g, of each coordination polyhedron, which can be defined by $f_g = [(3N_V - 6) - N_b]$. Here, $3N_v$ is the degree of freedom of N_V vertices of the polyhedron, and N_b is number of fictive bonds. The packing of polyhedra is characterized by the soft percolation of cages, which allows further changes with decreasing temperature. The power spectrum of displacement of the central ion in the cage is found to be correlated with the fluctuation of N_b of cation-cation (or anion-anion) pairs in the polyhedron, although the effect from the coordination shells beyond the neighboring ions is not negligible. © 2015 AIP Publishing LLC. [http://dx.doi.org/10.1063/1.4918586]

I. INTRODUCTION

Molecular dynamics (MD) simulations play significant roles to understand the slow dynamics and structures related to the glass transitions. Angell has introduced a concept of "fragile" and "strong" to characterize the dynamic of glass forming materials.[1] The former shows non-Arrhenius behavior of the dynamics, while the latter shows Arrhenius behavior. In the former, the T_g-scaled temperature dependence of structural relaxation time or transport coefficient has steep slope at $T_g/T = 1$ and the fragility is defined by the slope. There are other glass-formers having properties that are intermediate between the strong and fragile extremes. The dynamics and thermodynamic properties of strong and fragile glass-formers are very different, although glass transition is a common property. Ionic liquid (IL) is a suitable system to examine the glass transition in fragile liquids, because it is liquid over wide tempera-

ture range and it can be vitrified at sufficiently low temperature or elevated pressure. Therefore, ILs offer new materials for the study of structural relaxation and glass transition.[2]

To understand the mechanism of glass transition, one may assume the formation of infinitive network of some structural or dynamical units or domains at T_g, but it is not clear what is the length scale of the structural units that characterizes the glass transition. Often, either divergent or monotonically increasing dynamic length scales with decreasing temperature are considered as the primary cause[3–7] of glass transition. In spite of efforts over the past decades, there is no report of direct observation of divergence of the length scale so far. As to be discussed later, the connection of length scale with transport properties of the system is not direct. It has been argued that one should consider the length scale of the fluctuation because of the lack of the static length scales. However, this argument is not necessarily justified when many kinds of infinitive networks can be defined in the real space.[8–22]

In looking for an alternative way to understand glass transition based on the concept that is common to all glass-formers

---

a)Author to whom correspondence should be addressed. Electronic mail: habasaki.j.aa@m.titech.ac.jp

irrespective of whether they are fragile, intermediate, or strong, the approach of this paper was taken. Silica is a typical strong glass-former structurally described by the three dimensional networks. Motivated by this, we consider in analogy networks in fragile systems connected by bonds and/or cages. Generally, dynamics revealed by the intermediate scattering function, or equivalently the mean squared displacements of molecules in glass forming systems, and ions in ionically conducting systems, started at short times from the caged dynamics, subsequently changed to the sub-linear diffusive dynamics at intermediate times, and finally ended with steady state diffusion at long times. The cages (coordination polyhedra) are connected to each other to form networks. Therefore, even for the fragile system, one can consider the topology of this kind of network representing the packing of the cages. They are naturally correlated with the volume as well as the dynamics of the system.

It is difficult to say unequivocally that any arbitrary chosen network of mobile or immobile regions is responsible for the glass transition *a priori*. It is necessary to show how the network is related to the characteristics of glass transition such as transport properties, system volume, and thermodynamic properties. To accomplish this task, the transport properties, the components of potential energies, and the system volume are examined in the present work by molecular dynamics simulations, as well as structural changes related to the networks. The existence of the infinitive network of bonds and cages is then used to characterize glass transition in a fragile system. The system examined in the present work is the archetypal ionic liquid (1-ethyl-3-methyl imidazolium nitrate, EMIM-NO$_3$), which is ionically conducting and also glass forming.[2] Physics deduced from the simulations is expected to be generally applicable to ionic conductors and glass-forming systems, and can be used to bridge the two research fields.

The purpose of the present work on structure and networks is threefold. Generally, change of dynamics and thermodynamic properties are found at two characteristic temperatures, T_B and T_g, with $T_B > T_g$, on decreasing temperature (or increasing pressure) towards vitrification of glass formers.[23] Therefore, the first purpose is to show the existence of the changes of network properties at T_B and T_g. The changes of the total number of bonds, N_B, for cation-anion and that for the fictive bonds of cation-cation (and anion-anion) pairs, to be defined later, are examined, and the existence of T_B (or T_c) and T_g that are related to change of network properties will be shown. The results indicate that vitrification at T_g is characterized by the saturation of the number N_B of cation-anion bonds (followed by saturation of the other kinds of bonds) with the corresponding decrease of the degrees of freedom of the system. While occurring at T_B are the changes in the number of bonds and the packing of cages within the overlapping networks. Related properties examined are diffusivity, partial potential energies, and system volume, determined at constant pressure and temperature conditions.

The second purpose is to characterize the cages, the local structures in the network, and their changes on decreasing temperature by using the coordination number, N_V, and the number of bonds, N_b, within the coordination polyhedron.

Previously, these values had been successfully used to characterize the caged ion dynamics as well as the glass transition in lithium silicate.[19–21] The Li silicate is more fragile than silica but is stronger than the present ionic liquid.[24]

The third purpose is to characterize the dynamic properties of trapped ion in the cage by using N_V and N_b. Spectra of the motion of the central ions are compared with those of the motion of the cage characterized by N_b. The two are comparable, although contribution from outer shells of the cages is not negligible.

The concepts of "fictive bonds" and packing of the polyhedra discussed in the present work seem to be rather general. This is because the concepts of network, packing, and geometrical degree of freedom discussed hold for many systems. In other ionic liquids, factors such as "shapes" (i.e., modification by long chains) or "size ratio" of cation and anion should be taken into account, because the packing is affected by them.

Ionic liquids like N,N,N,N-tetramethyl-ammonium dicyanamide (TMA-DCA) have restrained condensed phases characterized as plastic crystals.[25] Although our attention is focused on one glass forming ionic liquid in the present work, it is interesting to examine the applicability of these concepts to other systems or phases in the future.

II. BACKGROUNDS

In the present work, we shall show the percolation of bonds and cages in an ionic liquid. As backgrounds of the analyses used, we summarized the concept of rigidity percolation and results of our previous MD simulations of the lithium metasilicate glass, which show the role of cages (coordination polyhedra) and geometrical degree of freedom in the glass transition and the dynamics of ions.

A. The concept of rigidity percolation

Topological aspects of the glass structure formed after glass transition have been a subject of intense discussion in the literatures.[8–22,26–28] Phillips introduced the constraint theory[8] for SiO$_2$ and the binary and ternary chalcogenide glasses As$_2$Se$_3$ and Ge$_a$As$_b$Se$_c$ to address glass forming ability. The number of bond-stretching constraints per atom with average coordination number $\langle r \rangle$ is $\langle r \rangle/2$, and the number of bond-bending constraints is $2\langle r \rangle - 3$. The optimal glass-forming composition corresponds to $\langle r \rangle = 2.4$. Thorpe[9,10,27] reformulated the constraint theory as a problem of rigidity percolation. Rigid units can be bars and joints. In random networks, numerical calculations have shown that a floppy-to-rigid transition occurs when $\langle r \rangle$ increases to a value quite close to the predicted mean-field value of 2.40. Experimental confirmations of the transition suggested by Phillips and Thorpe in various ways have been found in binary (Ge or Si)$_x$Se$_{1-x}$ and ternary Ge$_a$As$_b$Se$_c$ glasses.[11–14] Approaches using Volonoi polyhedra and Delaunay triangles (in two dimensions) or the similar one using tetrahedra (in three dimensions) for the units of networks are also known,[16] and the former type of analysis is frequently applied to fragile systems. For the network forming systems, (Na$_2$O)$_x$(P$_2$O$_5$)$_{1-x}$, analysis was made of data from photon correlation spectroscopy at temperatures near the glass tran-

sition and for compositions extending from pure phosphorus pentoxide to the metaphosphate ($x = 0.5$).[26] Pure P_2O_5 forms a three-dimensional network and has $\langle r \rangle = 3$. On increasing Na_2O, $\langle r \rangle$ decreases monotonically to 2. The "fragility" index m when plotted against $\langle r \rangle$ also exhibits a very shallow minimum near $\langle r \rangle = 2.4$. Experimentally, existence of several regions in rigidity percolation has been reported. Boolchand has observed an intermediate phase in binary Ge-Se glass[28] by Raman scattering measurements, different from that of the simple rigidity percolation.

B. Caged ion dynamics and glass transition in Li metasilicates

In the previous works by Habasaki *et al.*,[19–21] coordination polyhedra in the typical ionically conducting glass, lithium metasilicate (Li_2SiO_3), which consists of both LiO_x and SiO_y ($x = 3–7$ and $y \approx 4$) units were examined by molecular dynamics simulations using an empirical model. Later, essential parts of the results were well reproduced and hence confirmed by using the *ab initio* MO based potential model.[29] The results are summarized here for explaining several concepts and as a background for comparing with ionic liquids.

Geometrical degree of freedom, f_g,[30] of each coordination polyhedron (Li ions surrounded by oxygen atoms) can be defined by $f_g = [(3N_V − 6) − N_b]$. Here, $3N_V$ is the degree of freedom of N_V vertices of the polyhedron in three dimensions, 6 is the degree of freedom for translational and rotational motion of the polyhedron. In other words, "$3N_V–6$" bonds are necessary to fix the shape of the polyhedron. The concept is schematically shown in Appendix A for the case of $N_V = 4$. For the lithium metasilicate, the number of vertices N_V surrounding each Li ion and the number of the fictive bonds (contact pairs) among oxygen atoms N_b of the coordination polyhedron were counted. Saturation of the coordinated structure near glass transition temperature, T_g, was found and characterized by N_V, and N_b,[19] showing the loss of f_g at T_g. Similar behavior was also observed for the SiO_4 units. That is, the changes of the geometrical degree of freedoms for both the network former and network modifier are found at the glass transition temperature, T_g.

The motion of Li ions in both the liquid state and glassy state was found to correlate well with that of the motion of the cage surrounding it.[20] Actually, the Li ion moves with the center of mass motion of the coordination polyhedron.[21] Therefore, naturally the connectivity of cages is related to the compressibility and dynamic properties of the whole system.

Dynamics in ionic liquids are similar[31] to structural relaxation in other glass forming materials and also to ionic conductivity relaxation and diffusion in ionically conducting glasses. The common behaviors include existence of caged dynamics manifested as the nearly constant loss (NCL) in the susceptibility spectra, the jump motions that are spatially and dynamically heterogeneity,[32–36] a stretched exponential correlation function for the conductivity relaxation, and other properties.

Similar analysis of cages and/or bonds of ions using N_V and N_b is applied to ionic liquids in the present work, and the results will be shown useful to understand the common behavior of the different systems.

III. METHODS

A. Molecular dynamics simulations

Simulations of a typical ionic liquid, EMIM-NO$_3$ have been done in a similar manner as the previous works[2] using an all-atom model. Networks and polyhedra are examined with respect to the positions of center of mass of cations and anions throughout the present work. We used the potential functions of the form

$$U(R) = \sum_{bonds} K_r(r - r_{eq})^2 + \sum_{angles} K_\theta(\theta - \theta_{eq})^2$$
$$+ \sum_{dihedrals} \frac{V_n}{2}(1 + \cos[n\phi - \gamma])$$
$$+ \sum_{i<j}^{atoms} (\frac{A_{ij}}{R_{ij}^{12}} - \frac{B_{ij}}{R_{ij}^6}) + \sum_{i<j}^{atoms} \frac{q_i q_j}{\varepsilon R_{ij}}. \quad (1)$$

It is the sum of bond, angle, and dihedral deformation energies, pairwise standard (6,12) Lennard-Jones (LJ) potential representing the repulsive term and the van der Waals interactions, and the Coulombic interactions between atoms with charges q_i. The simulations were carried out by using the General Amber Force Field (GAFF)[37] and the program Amber.[38]

The system contains 256 EMIM$^+$ and 256 NO$_3^-$ with a total of 5888 atoms. Periodic boundary conditions were imposed, and Coulomb interactions were calculated using the particle mesh Ewald method. The system was equilibrated at 1000 K, and the temperature was gradually decreased in time steps. Each step was either 1 or 2 fs, and the simulations of NPT ensemble were carried out up to 2.5–10 ns after sufficiently long equilibration time of several ns. The cooling rate used is about 0.01 K/ps.

Topological examination of the system and polyhedra was performed typically at the onset time, t_{dif}, of the diffusive regime shown by the mean squared displacement (MSD), which corresponds to the time scale of the process contributing to the diffusion coefficient at each temperature. Notwithstanding, the essential features of networks obtained during $t \sim t_{dif}$ can be observed already from the instantaneous structure.

IV. RESULTS AND DISCUSSION

A. Structures of networks and cages—multiple character of networks

Characteristics of the networks are closely related to the length scales existing in the system. There are different kinds of length scales[39] considered so far in the problem of glass transition. Previously, we examined[40] the present EMIM-NO$_3$ ionic liquid by MD simulations[40] and have shown that there are several length scales[41] in the density distribution function and in the charge density distribution function of the system. The length scale of the density distribution function was found to be shorter than the charge density distribution function. These length scales are fundamental for considering the structure of the ionic liquid, although no divergence of the length scale was found near the glass transition regimes. Instead, one can consider the infinite connections among the cages or bonds to characterize these structures.

In Fig. 1, three instantaneous network structures are shown for EMIM-NO$_3$ in the glassy state (at 150 K), where the nodes are the center of mass positions of ions (blue: EMIM$^+$ ion and red: NO$_3^-$ ions), and bonds are connecting ions within the distance of the first $g(r)_{min}$. In Fig. 1(a), the neighboring cation-anion is connected and coordination polyhedra (anions surrounding cation) are shown. In Fig. 1(b), neighboring anions are connected. This partial structure is incorporated with the network formed by cation-cation pairs as shown in Fig. 1(c). These networks consist of well packed cages in the glassy states. The cause of the multiplicity of networks is
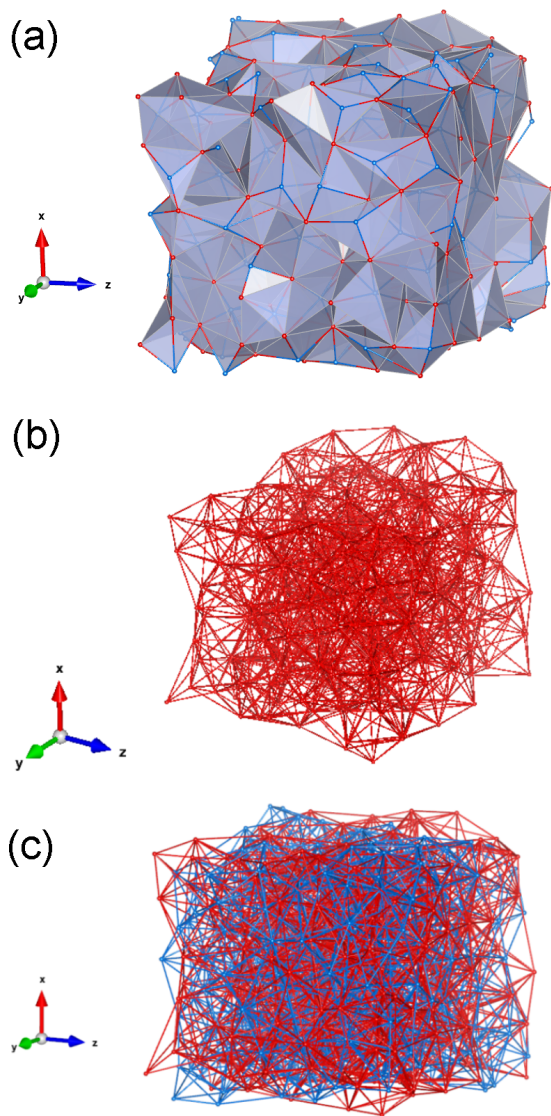

schematical represented in Fig. 2 for both the ionic and neutral systems. In this figure, the concept of overlap of polyhedra (networks) in the system is illustrated in 2D. In the upper example, overlap of the coordination polyhedra in binary (red and blue) system is shown. Red particle is surrounded by blue ones and vice versa. Therefore, these polyhedra are mixed together. One can imagine this situation as a binary mixture of different kinds of atoms, or a mixture of cation and anion. Thus, the networks formed by different kinds of ion pairs are mixing. This complexity with variety of the substructures is characteristic of the structure of ionic liquid such as EMIM-NO$_3$ and enhances anharmonicity of the dynamically formed cages. Examples of structures of clusters (within $g(r)_{min} = 7$ Å from the central cation) are shown in Appendix B for two cases near T_B.

Generally speaking, mixing of networks exists for fragile systems including non-ionic systems. In the example at the lower part of Fig. 2, overlap of coordination polyhedra is shown for two central particles in the one component system. The similar configurations of particles as in the upper part are considered there. In this case, a trapped particle is the same kind as the surrounding particles, and in turn, it can form a cage of the other particles. That is, even in the one component system, distinguishable substructures are found and the system can show the glass transition.[42]

FIG. 1. (a) Structure of the networks found in the glassy state of EMIM-NO$_3$ at 150 K (based on the full atomistic MD consists of 5888 atoms (256 ion pairs)). (a) Positions of the center of mass of anions (NO$_3^-$: red) and surrounding cations (EMIM$^+$: blue) within the distance of $g(r)_{min}$ of cation-anion pair are connected, and the coordination polyhedron (anions around cation) was visualized. All neighboring cation-anion (ionic) bonds are shown here. The structure is repeated by the periodic boundary condition applied to form an infinite network. (b) The same structure as in (a), where the positions of center of the mass within $g(r)_{min}$ of neighboring anion-anion pairs are connected (red lines). (c) The same structure as in (a) and (b), where substructures of cation-cation network (blue lines) and anion-anion network (red lines) are overlapping. The latter is the same as in (b). Thus, fragile system consists of overlapping networks with distribution of coordination numbers.
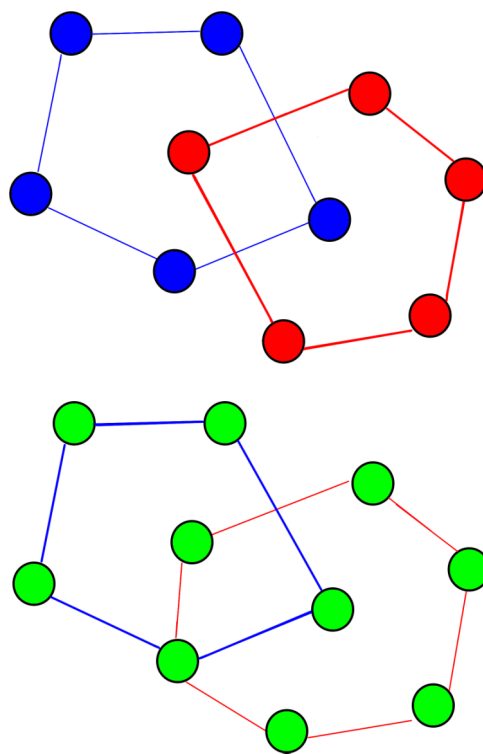
FIG. 2. Concept of overlap of polyhedra (networks) in fragile system represented in 2D. (Upper case) Overlap of the coordination polyhedra in the binary (red and blue) system is shown. One can imagine this as a mixture of different kinds of atoms, or a mixture of cation and anion. (Lower case) Overlap of coordination polyhedra is shown for two central particles in one component system. Although the similar configurations of particles are considered in both cases, network considered can be different by the definition of polyhedron.

The concept of soft percolation concerned with mixing of networks will be introduced later on to explain the behavior of the fragile ionic liquid (EMIM-NO$_3$). In Sec. IV B, temperature dependence of the structural properties of the IL will be examined based on the pair correlation function, $g(r)$.

B. Characteristics of structures and dynamics of the ionic liquid

Ionic structure of EMIM-NO$_3$ was examined at several temperatures from the pair correlation functions $g(r)$ shown in Fig. 3. At the first glance, the shapes of all $g(r)$ are similar. However, there are changes in the coordination number as well as the number of "fictive" bonds on decreasing temperature. The first peak from cation-anion pairs increases at first and then becomes saturated. The shoulder at around 4 Å from the cation-cation pairs and that at around 9 Å from the anion-anion pairs both become clearer below 400 K. The first peak of anion-anion pairs is sharpened and shifted to shorter distance at around this temperature. When the system is deeply cooled down to below T_g, some fine structures in $g(r)$ appear, including those from the cation-anion pairs due to localization by vitrification.

Since changes of the first minimum position are relatively small, we used fixed cutoff values to determine the bonds of network and polyhedra. Namely, the first minimum positions of $g(r)$ at 7 Å, 10 Å, and 11 Å were used for the cation-anion, anion-anion, and cation-cation pairs, respectively. In the present work, we distinguish the total number of bonds, N_B, counted without redundancy for the system from the number of bonds, N_b, in each polyhedra, which have a redundancy with other polyhedra. Therefore, usually, $N_B < \sum N_b$.

C. Existence of T_B and T_g in the dynamics of ionic liquid

Before examining the details of the network structures, existence of the two characteristic temperatures relevant to characterize the changes of dynamics of the system will be shown.[23,42]

Previously, Xu et al.[43] examined viscosity and conductivity of ionic liquids for old and unpublished data with quaternary ammonium cations and new data on salts of aromatic cations containing a variety of anions, and the results show wide range of liquid fragilities. Khupse and Kumer[44] examined the fragile behaviors of viscosity of binary mixtures of pyridinium based ionic liquids and discussed the effect of mixing with solvent. Our diffusion coefficient data can be fitted to Vogel-Fulcher-Tamman-Hesse (VFTH) equation, and the fragile behaviors found in the diffusivity of the present system are consistent with the temperature dependence of viscosity or conductivities of these related ionic liquids.

Temperature dependence of the diffusion coefficients of the cation in the present system, which were obtained from the mean squared displacements in the diffusive regimes via the Einstein equation, is shown in Fig. 4. The diffusion coefficients at 400 K obtained for the same system (by MD with different models) by Popolo et al. and Yan et al.[45,46] are also shown in the figure for the sake of comparison.

Although our diffusion coefficient data can be fitted to the VFTH equation, fits to Arrhenius temperature dependence also hold separately at temperatures above and below 410 K. The presence of clear inflection in the plot of logarithm of the diffusion coefficient against $1/T$ is assigned as T_B. In this sense, fragile behavior is characterized by the slower decrease of the diffusion coefficient at higher temperature region above T_B, and the change to a more rapid decrease below T_B, instead
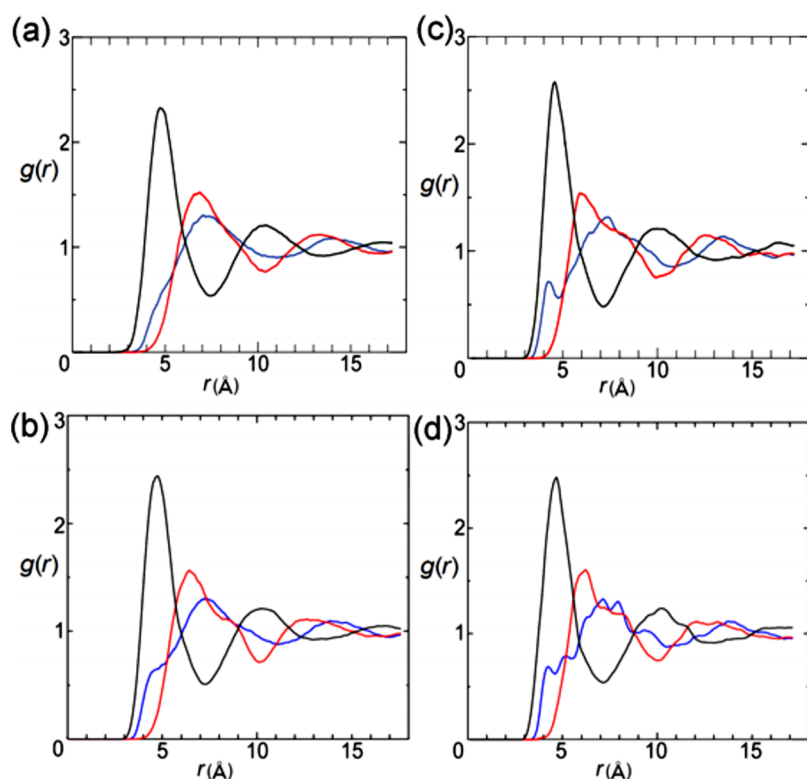

FIG. 3. Pair correlation function of EMIM-NO$_3$, examined for the center of mass position of the ions. Black: cation-anion, red: anion-anion, and blue: cation-cation. (a) At 600 K, (b) at 400 K, (c) at 250 K, and (d) at 150 K.
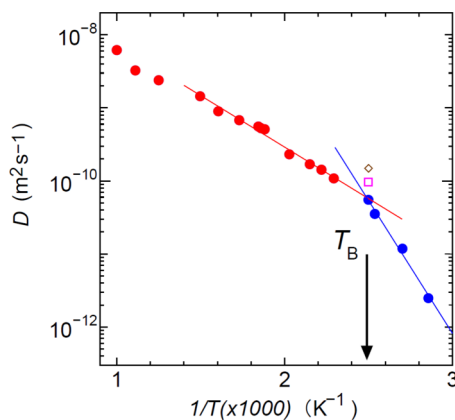
FIG. 4. Temperature dependence of diffusion coefficient of the cation. Although this can be well fitted to the VFTH function, it can also be well fitted to two exponentials (or two power laws). An inflection was found at around $T_B \sim 410$ K. At around this temperature, the distribution of N_b changes. That is, the structure with $N_b < (3N_V - 6)$ found at higher temperature disappeared on crossing T_B (see Figs. 8 and 9). The structure with $N_V = 4$ also disappeared. The inflection temperature T_B is considerably higher than T_g (~ 250 K) and has a high diffusivity and is measurable within $\sim$ns runs in MD. Open square (pink) and open diamond (brown) marks are shown for the sake of comparison, which were obtained by non-polarizable and polarizable models of previous MD works,[45,46] respectively. Approximate positions of T_B and T_g are shown in Figures 4–6, except for T_g for the diffusion coefficient, for which diffusive region was not attained during the observation time.

of the rapid increase of the T_g-scaled transport coefficient on decreasing temperature towards T_g. Diffusivity near the inflection point (~ 410 K) is of the order of 10^{-10} m^2/s and is measurable within $\sim$ns runs. While at T_g (~ 250 K) determined by change of the temperature dependence of the density, diffusive regime of MSD was not attained during the observation time. The kinetic glass transition temperature, $T_{g\text{-}k}$, obtained from simulations up to ~ 10 ns by the condition that the diffusive regime is not attained during the observation time, is higher than $T_g = 250$ K but lower than T_B. The behavior of the anions is similar to cations[2] because of comparable effective sizes.

Previously, the change of diffusivity at T_B was discussed[2(b)] to be related to fractal dimension of the random walks, d_w,[47] which is a measure of the complexity of the trajectory. This result is summarized here.

For the determination of d_w, how many times (N') required to cover the trajectories was counted with changing the length of the ruler (L). From the slope in the double logarithm plots of N' against L, one can determine the fractal dimension of random walk, d_w, defined by

$$N' = AL^{-d_w}. \qquad (2)$$

Two regions of slopes for short and long range motions were found. The d_w was found to increase rapidly after T_B, with decreasing temperatures. Namely, above T_B, the motion is dominated by the long range and/or forward correlated motions with a small d_w, while below T_B, the motion is short ranged with a large d_w, which indicates strong back-correlated motions of the ions. The strong increase of d_w value is related to the decrease of the free volume available for the motion, and this result is consistent with the changes in network structures, which will be discussed in the present work.

D. Existence of T_B and T_g in the system volume and potential energies in the ionic liquid

Since possible change in the system volume at around T_B (~ 410 K) was expected, we have examined the temperature dependence of volume of the system by providing more data points at around this temperature than the previous work. The data were obtained by MD simulations in NPT conditions at each temperature after equilibration. When plotting volume against reciprocal temperature, changes in the slope at around ~ 410 K and ~ 250 K are found as shown in Fig. 5(a). Experimental value at 293 K by Cang et al.[48] is also shown in this figure as well as the MD data at 400 K in Refs. 45 and 46 for the sake of comparison. In Fig. 5(b), partial potential energies of the system are shown for each term appearing in Eq. (1). The energies are shown as relative ones obtained by subtracting the values at 600 K. Except for the Coulombic and the LJ terms, they are for the inner structures
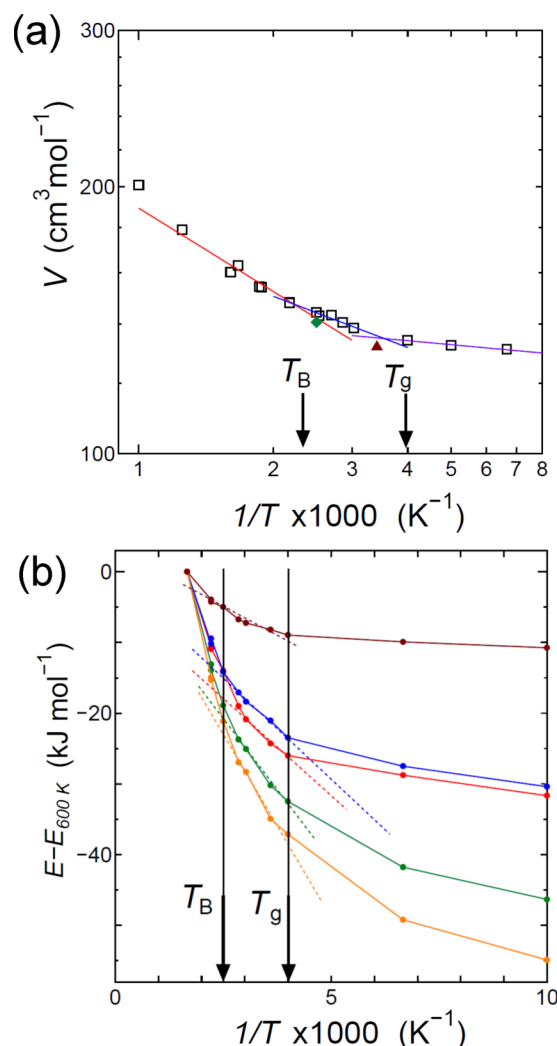

FIG. 5. (a) Temperature dependence of volume of the system obtained by this MD work. Lines are fitted ones using power laws for three temperature regions. Error is within the size of the mark. Red: above T_B, blue: between T_B and T_g, purple: below T_g. Filled diamond (green) is obtained by MD[45,46] using different models (two points are overlapped). Filled triangle (brown) is an experimental value.[48] (b) Relative changes (measured from 600 K) of partial potential energies of the system. Brown: dihedral angular, blue: LJ, Red: Coulombic, green: bonding, and orange: angular terms. Dotted lines are used to show the slope in the intermediate regions between T_B and T_g.

of ions. Two inflections at temperatures T_B and T_g are observed for all of these terms. The changes of bonding and angular energies for the inner structures have large contribution for the stabilization of the system with decreasing temperature. However, for these terms, the inflections are not that clear as compared with the other terms. Nearly flat behaviors are observed for the Coulombic and dihedral angular terms at temperatures lower than T_g. The trend means the importance of the ion-ion structure as well as the medium and longer length scale structures related to the dihedral angle in regard to glass transition. Thus, the existence of both characteristic temperatures was confirmed in dynamics, density, and potential energies. In Sec. IV E, corresponding changes in the whole system is characterized by the network formed by "bonds."

E. Number of bonds and degree of freedom for the whole system

The degrees of freedom of the system consisting of N particles, F_{system}, can be defined by

$$F_{system} = [(3N - 6) - N_B].   (3)$$

Here, counting is taken over all bonds (contact pairs) without redundancy. For N particles in 3 dimensions, $3N$ is the degrees of freedom of the motion, and 6 is that for the rotational and translational motion of the system. Then, the probability P of finding a mode with $N_B < 3N$-6 is defined by

$$P = F_{system}/(3N - 6) = 1 - \frac{N_B}{(3N - 6)}.   (4)$$

The probability of finding a part without the mode is the complement,

$$1 - P = \frac{N_B}{(3N - 6)}.   (5)$$

If the value exceeds 1, it means that the inner structures of the system have extra bonding compared with the value of $3N - 6$. In the present work, analysis has been done for each combination of the pairs of species. The results of $1 - P$ plotted against the inverse of temperatures for cation-anion, anion-anion, and cation-cation pairs are shown in Fig. 6. Here, N stands for the number of all ions, although the number of bonds is counted among the cations (or anions) in the case of cation-cation (anion-anion) pairs.

The interaction of the cation-anion is the strongest one in ionic liquids because of its shortest length, and the connection is by the attractive Coulombic force. While the interactions for other pairs are repulsive, and the bonds are fictive ones formed by the collective forces from other ions. Therefore, the trends observed for the three different combinations are similar, but not the same. When the temperature is decreased, changes at positions around $T_B \sim 410$ K are observed for the three networks. The positions seem to be slightly different for three cases. This feature is probably due to the soft character of the packing to be discussed later. The value of $1 - P$ and its change of slope for the cation-cation pair is the largest, and it seems to be natural in view of the packing of the bulky cation. Saturation of the value of $1 - P$ for all the three networks is
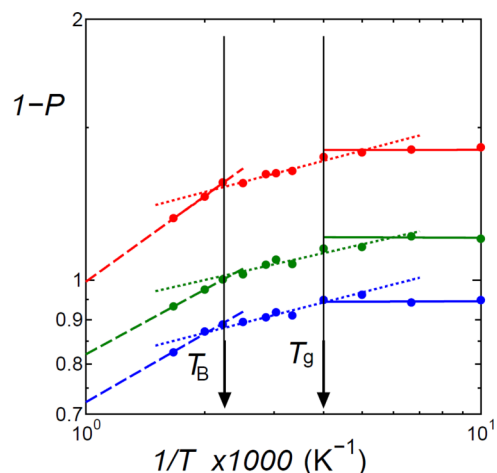

FIG. 6. The probability, $1 - P = \frac{N_B}{(3N - 6)}$, is shown as a function of reciprocal temperature, where the total number of bonds (contact pairs) within $g(r)_{min}$ of anion-cation (blue), anion-anion (green), and cation-cation (red) pairs is counted without redundancy. At around T_B (~410 K) and T_g (~250 K), the change of slopes for the three kinds of networks is observed. The saturation of the number of bonds is observed for the cation-anion network at around T_g and followed by others. Error bars estimated at 250 K from three independent cooling schedules are within the size of the mark. The data at $T = 0.1$ K were included in the fitting at the lowest temperature regions.

found at around 250 K, that is T_g. The saturated value for cation-anion network is near 1, and the saturation occurred prior to that for the other combinations. This finding suggests that even for a fragile system, glass transition can be described by the formation of rigid networks involving the strongest interactions at the shortest distance. For other combinations, even larger saturated values were observed. This is because fictive bonds examined are loose ones having several lengths. Thus, the changes in the network of the system are found at both T_B and T_g.

As discussed in Secs. IV F–IV L, the changes of the free volume of the system is related to these inflection points and the packing of coordination polyhedra.

F. Existence of T_B and T_g in the ionic liquid and relation to free volume

Decrease of the free volume in the system can be measured by the positronium annihilation lifetime spectroscopy (PALS).[49,50] Correlation of the free volume with the failure of a single VFTH expression to describe the temperature dependence of the structural α-relaxation time was found by PALS[50] in *ortho*-terphenyl and propylene carbonate, glycerol, and propylene glycol. Recently, Forero-Martinez *et al.*[51] have examined voids in three ionic liquids ([C$_4$mim][PF$_6$], [C$_4$mim][Tf$_2$N], and [C$_3$mim][Tf$_2$N]) by MD simulations. The trend observed in PALS[52] was reproduced by MD. Although T_g by their definition seems to lie between T_B and T_g according to our definition, their observation of the temperature dependence of volume shows the existence of the intermediate temperature region as in this work.

The following analysis of the polyhedra presented is concerned with how the free volume is located in the system, and reduced on decreasing temperature.

G. Temperature dependence of the distributions of N_V and N_b

The polyhedron of anions surrounding cation and vice versa also was examined as was done before in the Li metasilicates.[19–21] The cutoff distance previously mentioned was used. In this definition of the coordination polyhedron, the mobility of trapped particle and cages is closely connected, and the size of the polyhedra is larger than the Delauny tetrahedra or Voronoi polyhedra. Structural change accompanying glass transition is sometimes not emphasized in the study of glass transition. However, in the distribution of N_V and N_b, one can clearly observe the change in the structure at both T_B and T_g. To characterize the local and medium range packing, we considered coordination polyhedra of anions around cation and cations around anion. The distribution of coordination number, N_V, at 600 K, 400 K, and 150 K for the anions around cation are shown in Fig. 7. Peak position tends to increase with decreasing temperature. Contribution of $N_V = 4$ is almost totally missing below 400 K. The distribution at higher temperature has a tail of larger N_V values, while in the glassy state at 150 K, the distribution is rather symmetrical and centered at $N_V = 7$.

Since the number of ions does not change with temperature, the increased number of N_V with decreasing temperature means the increased overlaps of cages and redundant counting of vertices or edges of polyhedra. In other words, the free volume of the systems decreased with such overlaps and with the reconstruction of polyhedra and networks. This reconstruction seems to be suppressed at temperatures below T_B.

H. Changes of the distribution of N_V and N_b at around T_B and T_g

In this section, temperature dependence of the packing of cages is examined by using N_V and N_b values to understand the structural changes at two characteristic temperatures, T_B and T_g. Probability distribution, P, of N_b is shown in Fig. 8 for temperatures at 600 K, 450 K, 400 K, 300 K, 250 K, and 150 K. The lines are drawn to serve as interpolations. Fig. 9 shows a comparison of these distributions at the different temperatures using the same color codes as in Fig. 8. Changes of the distributions at both T_B and T_g can be seen. Large change of the distribution pattern related to the increase of N_V and N_b values in each peak is found at temperatures higher than T_B. Below T_g, the pattern is similar except for small sharpening at large N_b value. Between T_B and T_g, gradual increase of N_b within each peak occurs with a small shift in N_V.

The change at T_B is related to the disappearance of polyhedra with $N_b < (3N_V - 6)$, characterized by this degree of freedom (see also Fig. 10). Because of the existence of redundant bonds, ($N_B < \sum N_b$), the loss of the geometrical degree of freedom for the coordination polyhedra occurs before T_g.

Positions of peaks in Fig. 8 are informative for learning what geometrical rule governs the packing of ions. At 600 K, the peak positions are at N_b equals to 6, 9, 13, 17, 22.5, and 27 (for $N_V = 4$–9), while at 400 K, they are at N_b equals to 6, 9, 13.5, 17.5, 21.5, and 26.5 (for $N_V = 5$–9). At 150 K for the glass, peaks are located at N_b equal to 10, 14, 18, 22, and 28 (for $N_V = 5$–9). At higher temperature, the differences between successive peaks of N_b are 3, 4, 4, 5.5, and 4.5. At and near the
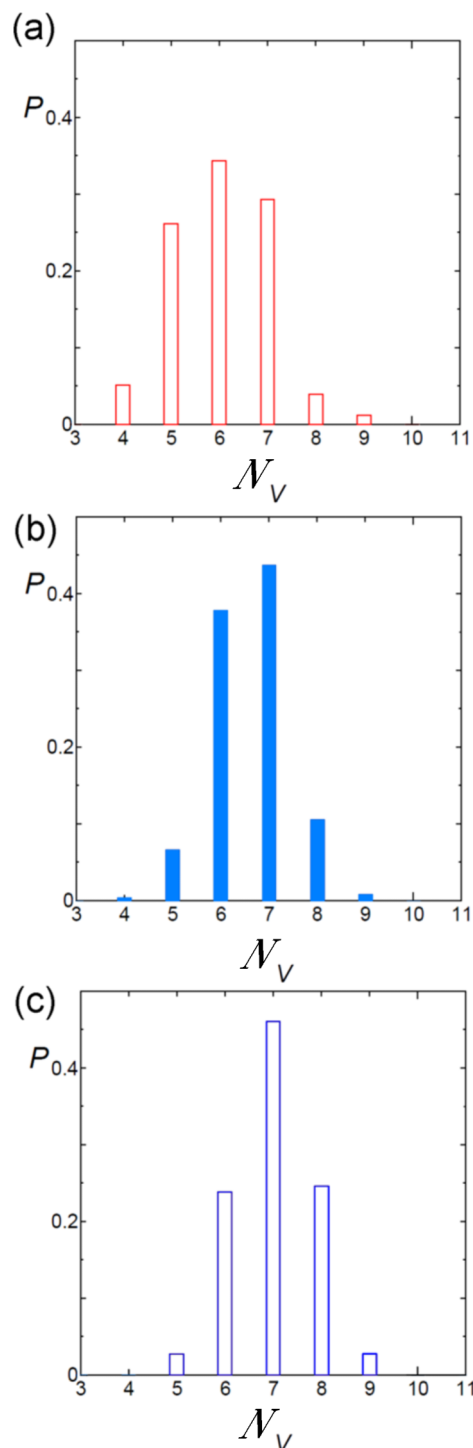

FIG. 7. (a) Distribution of vertices of polyhedra formed by anions around cation at 600 K in EMIM-NO$_3$. (b) The distribution at 400 K. (c) The distribution at 150 K.

T_B, the differences change to 3, 4.5, 4, 4, and 5, while in the glassy state at 150 K, the values are 4, 4, 4, and 6. In the case of the geometrical degree of freedom is equal to 0, the N_b value increases by 3 with the addition of each vertex. Therefore, the difference between successive peaks (i.e., the peak interval) of three is expected. Although an inflection of the temperature dependence of the diffusion coefficient at around 400 K can be well explained by the loss of structures with $N_b < (3N_v - 6)$, the different rule with the peak interval equal to 4 appeared
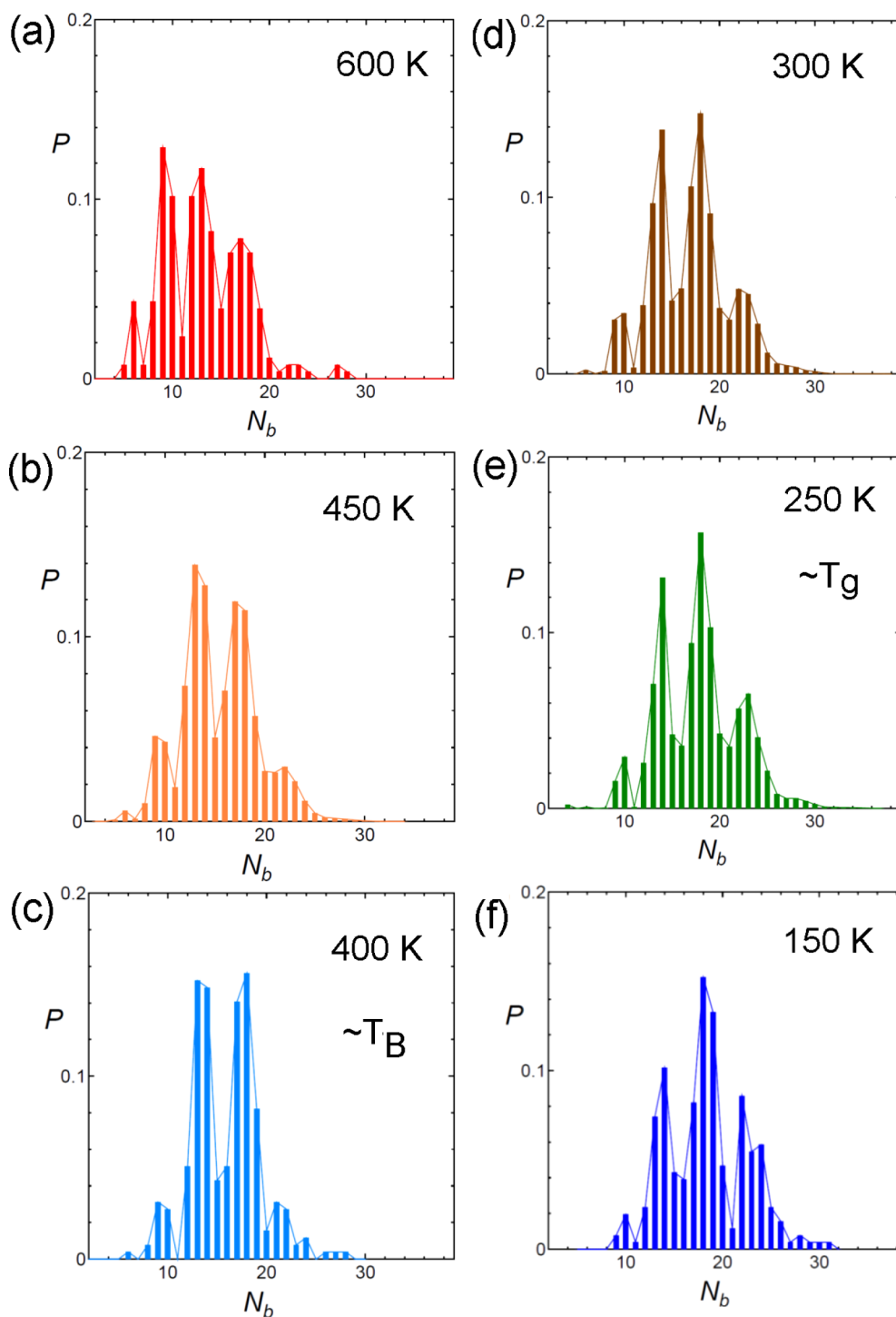
FIG. 8. (a) Distribution of number of fictive bonds N_b of anion-anion in the coordination polyhedral of anions around cation at 600 K (red) in EMIM-NO$_3$. (b) The distribution at 450 K (orange), (c) at 400 K (pale blue), (d) at 300 K (brown), (e) at 250 K (green), and (f) at 150 K (blue). The peak at around $N_b = 6$ is for $N_V = 4$ and this contribution is almost missing below T_B. Each peak maximum corresponds for N_V shown in Fig. 8, but the region shows some overlaps as will be shown in Fig. 10. The values are connected by lines of the same color and they are compared in Fig. 9.

with further decrease of the temperature. Related to this feature with peak interval of 4 is the existence of a plate consisting of two cation-anion pairs, and combinations of them. They do not necessarily show an anti-parallel arrangement to compensate for a charge of the plane. Another characteristic structure found is a plate (6-member ring) formed by three cation-anion-pairs. The structure near the glass transition temperature contains the connection of these plates. Even at this temperature, a

bond (cation-anion connection) is not completely rigid, and a central ion has a local mobility, as shown later for the spectra or fluctuation of N_b and the absolute value of the displacement of ith-ion, $|r_i|$.

Although the peak position in Fig. 8 corresponds to each N_V, some overlaps of the regions of N_b values exist. This situation is shown in Fig. 10. In this figure, the combinations of N_V and N_b observed are shown by circles. The dotted
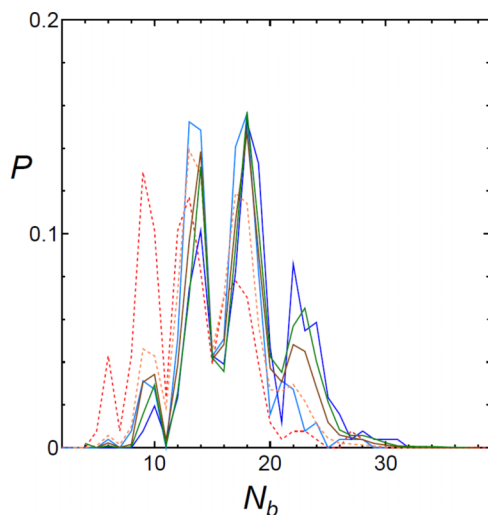
FIG. 9. Comparison of the distributions in Fig. 8. The same color for each temperature as in Fig. 8 is used. Dotted ones are for the system above T_B, where the contributions of small N_V values and small N_b values in larger N_V region are observed.

curve connects the approximate positions of the peak maxima of N_b value for different N_V. The lower blue line stands for $N_b = (3N_V - 6)$. That is, on this line, the geometrical degree of freedom is equal to 0, and the shape of the polyhedron is fixed. The upper curve (red) stands for $(1/2)N_V(N_V - 1)$, which is the maximum number of bonds for each polyhedron. Even if each cage had enough number of bonds to stabilize the shape of the structure, further increase of fictive bonds is allowed below T_B. Here, the number of N_b is counted by the pairs with distance less than the position of $g(r)_{min}$ for the anion-anion pair (=10 Å). The peak in $g(r)$ for the first shell is broad and has several shoulders. Therefore, the fictive bonds are loose ones having several lengths, and it is not surprising that the number can be near the upper limit. At 600 K, some points are located below the blue curve. This contribution is still observed at 450 K, just above T_B. These points are polyhedra with $(3N_V - 6) > N_b$, each of which is having a free space between anions. At 400 K and 150 K, such structures are not observed except for minor contribution of $N_V = 5$ and $N_b = 8$ at 400 K, and of $N_V = 6$ and $N_b = 11$ at 150 K. Therefore, above $T_B \sim 400$ K, there is a geometrical degree of the freedom for polyhedra, and the change in the structure is accompanied by the decrease in the free volume with increase of N_b and N_V. Below $T_B \sim 400$ K, the change is mainly in the distribution in N_b and N_V of the polyhedra within the limited region of N_v, and within the region between the two limiting curves. This change of structure with temperature is consistent with the trend found in the slopes of diffusion coefficient on crossing 400 K shown in Fig. 4. Below T_g, the change of the pattern of distribution is small and the sharpening of each peak is the dominant effect.

To characterize the packing, we also considered coordination polyhedra of cations around anion. Temperature dependence of N_b distribution is shown in Fig. 11 for three temperatures, 600, 400, and 150 K. Although the trend is similar to the other case presented in Fig. 8, some differences are found. The peaks are sharper and seem to be more separated with $\delta N_b \sim 5$. The structure with $N_b < (3N_V - 6)$ was not so clear at the high temperature region. Such differences in the mutual
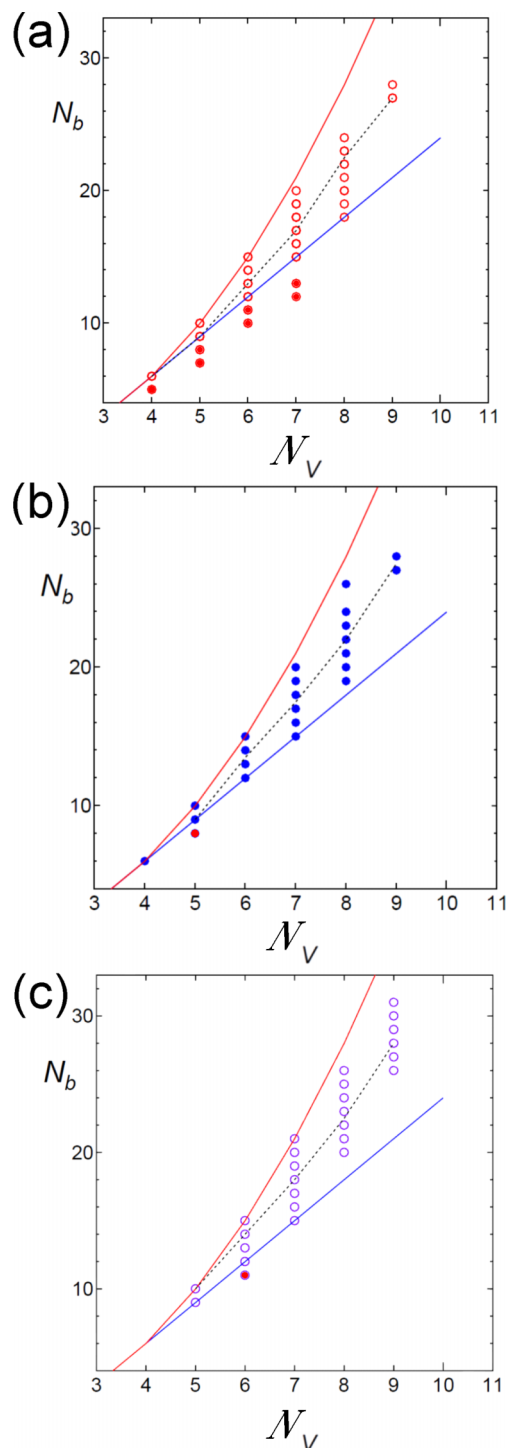

FIG. 10. Relation of N_b and N_V for (a) 600 K, (b) 400 K, and (c) 150 K. Dotted curves are connecting the approximate peak positions of the distributions of N_b shown in Fig. 8. Blue curves are for $N_b = (3N_V - 6)$ structures, meaning the loss of geometrical degree of freedom. Red curves are for $N_b = (1/2)N_V(N_V - 1)$). Below 400 K, the data located within these curves stand for strained structures and the structural changes occurred mainly by the slightly increasing N_b values in larger N_V structures. This structure at 400 K or below it allows a diffusive jump motion of ions as shown in Fig. 4. In these figures, polyhedra with $N_b < 3N_V - 6$, below the blue curve are shown by filled red circles.

coordination will become more important when the difference between the effective sizes of cation and anion becomes larger, although the MSD^2 of cations is comparable to that of anion in our model system.
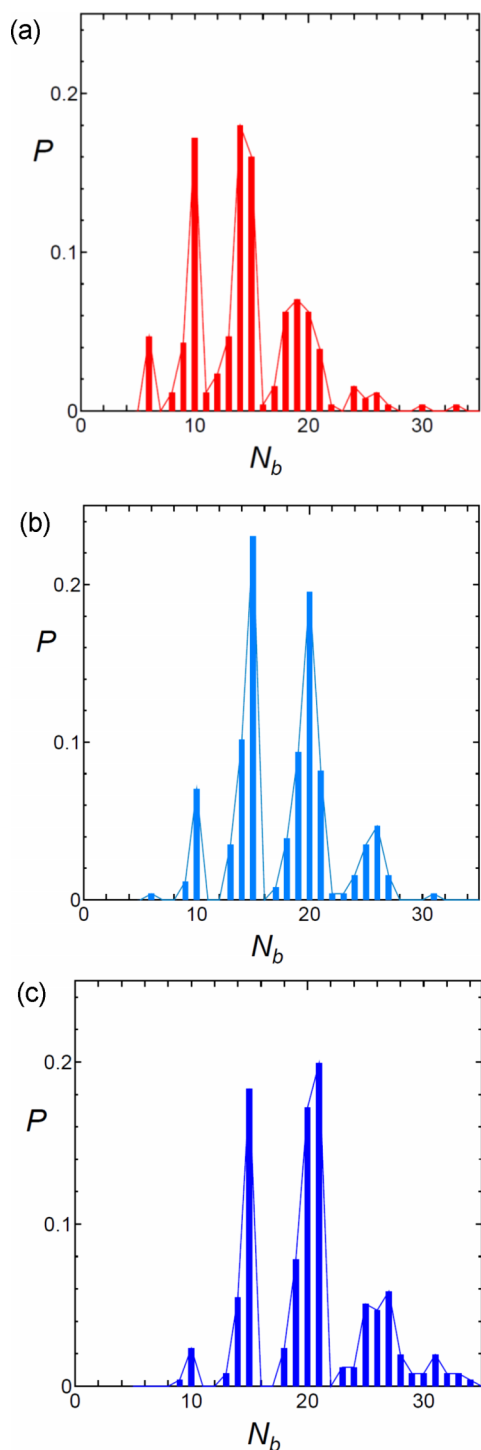
FIG. 11. (a) Distribution of number of fictive bonds N_b of cation-cation in the coordination polyhedral of cations around anion at 600 K in EMIM-NO$_3$. (b) The distribution at 400 K. (c) The distribution at 150 K. Color code used is the same as in Fig. 8 for these three temperatures. The trend of temperature dependence is similar to that in Fig. 8 but the peaks are more separated and sharper.

In the present work, we used the center of mass positions of ions for analysis, because it seems to be better than the center of charges to consider the packing of the structures. If ion is more asymmetrical or having long tails, the different treatment of the positions and/or shapes may be required, because it affects the packing in the system.

Temperature dependence of the characteristics of the polyhedra is shown for the anions around cation. In Fig. 12, blue polyhedra have a character with $N_b < (3N_V - 6)$. Yellow ones are for the structure with $N_b = (3N_V - 6)$, while green ones are for polyhedra with maximum number of bonds, $N_b = (1/2)N_V(N_V - 1)$. Gray ones are polyhedra with the N_b between $N_b = 3N_V - 6$ and $N_b = (1/2)N_V(N_V - 1)$. The contribution of the polyhedra with $N_b < (3N_V - 6)$ becomes negligibly small at T_B. This fact is clearer in Fig. 13, where the gray polyhedra are not shown. This result is consistent with the change of the compressibility of the system at around 400 K. Large N_b structures become dominant at lower temperatures. At T_g, the characteristics of polyhedra change again by the saturations of the shortest connections by the cation-anion pairs followed by the other pairs. Positions of polyhedra can change even below T_g by localized motions. These observations are also consistent with the trends observed in the total number of bonds of each pairs shown in Fig. 6.

I. The concept of soft percolation

In the case of ionic liquids, multiple networks make the system a complicated one. Namely, cages of anions are formed by cations, while the cages of cations are formed by anions and these networks are highly intertwined as already shown in Fig. 1 and schematically illustrated in Fig. 2. The first changes at T_B seem to be the characteristics of the fragile system, where the slope of the diffusivity changes. This is related to the packing of networks, and involves the changes of packing of coordination polyhedra around the anion or the cation.

The concept of percolation concerning a fictive bond (contact pair) is slightly different from the rigidity percolation involving direct bonding. We call it soft percolation and this effect can be described and explained as follows.

As already mentioned, fictive bonds are defined for the neighboring pairs of cation-cation (or anion-anion), where the interaction is via the repulsive force modified by the other terms of the potential. Such fictive bonds can increase even after the condition $N_b = (3N_V - 6)$ has been attained. As a result, gradual change of the topology of cages continues below T_B until the system has been deeply cooled. In other words, the volume of the system is reduced until the more rigid bonds by cation-anion interaction, which connects the loose networks of anion-anion and cation-cation, are formed. Often large coordination numbers and "fictive" bonds are found with the soft percolation. The large coordination number of the system and mixing of different networks mean the existence of variety of structures with different N_b and N_V. This will result in wide distributions of lifetimes of the structures as well.

The "soft percolation" characterizes the gradual changes in volume and the non-Arrhenius behavior of diffusivity in the fragile system.

On the other hand, in silica, the equality, $3N_V - 6 = (1/2)N_V(N_V - 1)$, for the tetrahedra holds, and therefore, further changes of the number of bonds in polyhedra are not allowed after the loss of geometrical degree of the freedom, and this explains the Arrhenius behavior of the strong system.
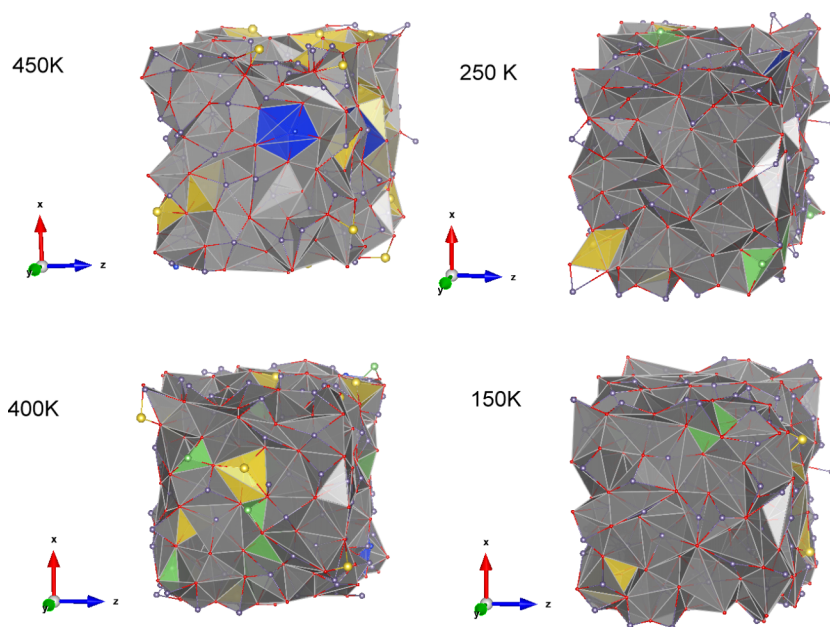
FIG. 12. Characteristics of coordination polyhedra of anions around cation. Blue: polyhedron with $N_b < 3N_V - 6$. Yellow: polyhedral with $N_b = 3N_V - 6$. Green: polyhedra with maximum number of bonds, $N_b = 1/2N_V(N_V - 1)$. Gray: between these characteristic numbers of N_b. The network of cages already exists at higher temperature than T_B. Bonds representing the cation and anion pairs interacting with Coulombic force.

J. Relation of the structure of polyhedron with the dynamics

Ion moves in conjunction with the deformation of the polyhedron characterized by N_b and N_V as found in previous works on the lithium silicate system.[19–21] Validity of this in the ionic liquid is examined here for several cases. Since motion of ions is dynamically heterogeneous, we have selected two typical cases taken near T_B with large and small displacements as shown in Appendix B.

Comparison of the power spectrum of N_b with that of $|r_i(t)|$ for these cases is informative. The correlation is clearly found in the power spectra by the multi-taper method (MTM)[53] determined from $|r_i(t)|$ of the central cation and $N_b(t)$ of the coordination polyhedron of anions surrounding it (see Fig. 14). The Nyquist frequency ($f = 0.5$) corresponds to $1/(2\delta t)$ (THz),

where $\delta t = 0.8$ (ps). The zero frequency mode corresponds to the diffusive motion, and the power law frequency dependence (caused by back correlated motion of ions) is found and observed at around $f = 0.002–0.03$, while the diffusive mode and power law region are naturally missing in the case of the localized ion. Comparison of these four cases has revealed that the main feature of the dynamics is determined by the changes in N_b (and N_V related to it) in the first approximation, but the effect from outer shells is not negligible for the motion of the central ion. In the case of localized ions, the motion tends to be suppressed by the outer shells, while the mobile ions tend to be further accelerated by them in these examples. This difference means that the heterogeneity of the dynamics is enhanced by the outer shells.

The other case examined is taken near T_g (see Appendix B and Fig. 15). Situation of an immobile cation at 250 K is similar
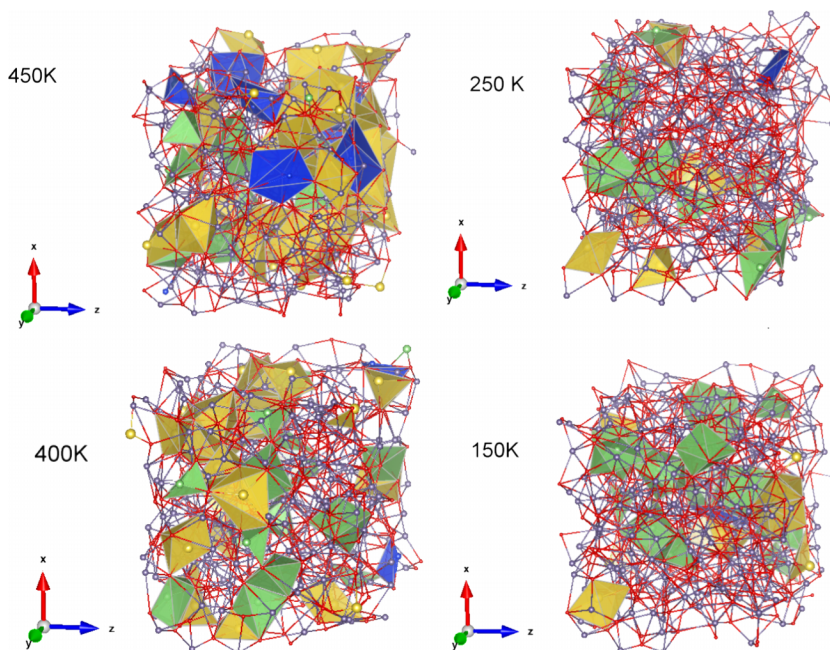

FIG. 13. Characteristics of coordination polyhedra of anions around cation. The figures are the same as Fig. 12, except for that gray ones between $N_b = 3N_V - 6$ and $N_b = (1/2)N_V(N_V - 1)$ are not shown. Decrease of the structure with $N_b < 3N_V - 6$, at around T_B becomes clearer. At the glass transition temperature ($\sim$250 K), the saturated N_b structures increase. The glass transition is also characterized by the saturation of total number of bonds of pairs in Fig. 6.
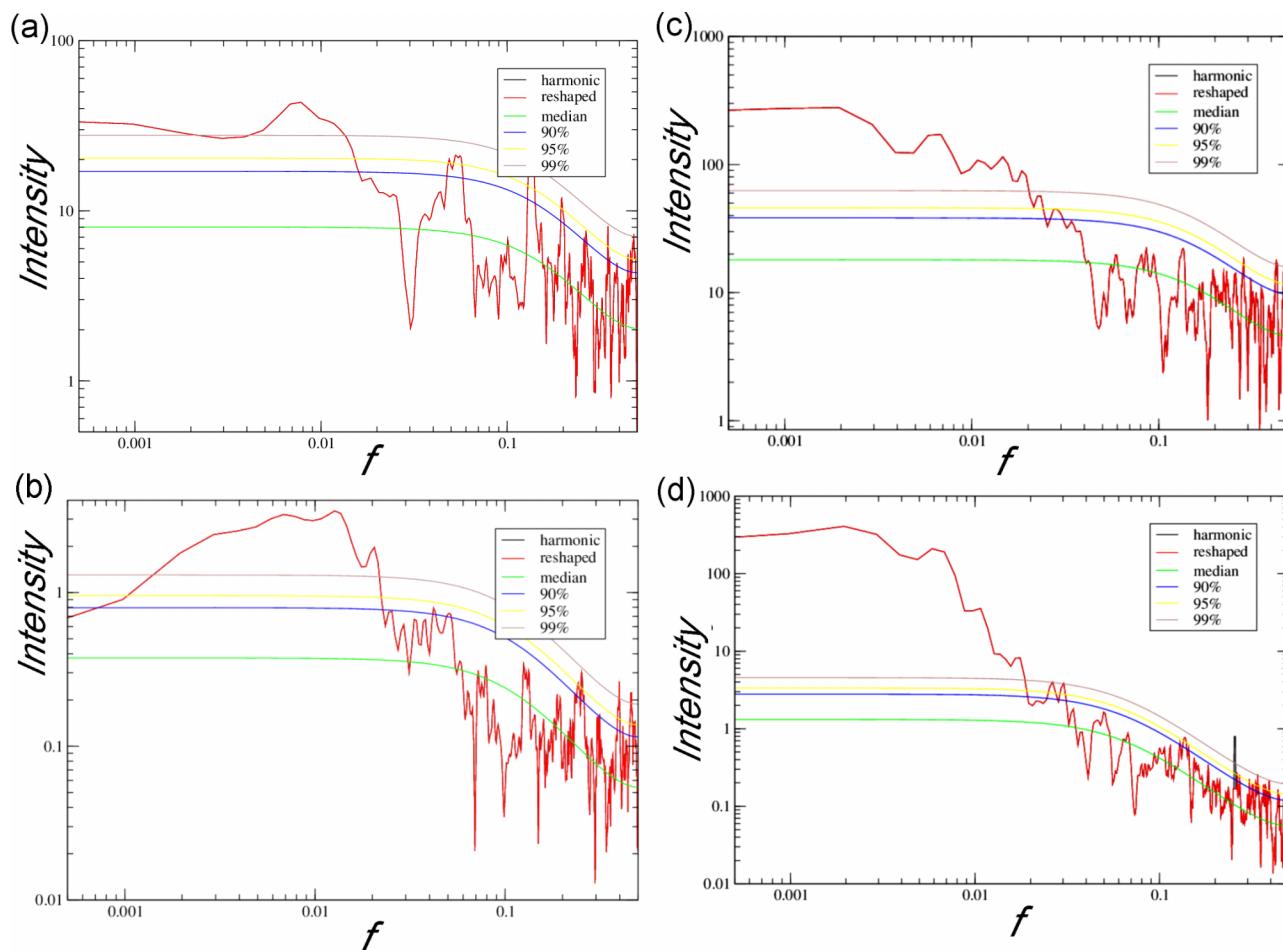
FIG. 14. (a) MTM power spectrum for the fluctuations of N_b values of the polyhedron of the anions around the localized cation was examined. Relatively larger intensity of the spectrum $f \sim 0$ is found for the fluctuation of N_b. (b) The spectrum of the displacement $|r_i(t)|$ of the central cation shown in (a). Power law region is not clear and the zero frequency mode is negligibly small for the displacement. (c) The MTM power spectrum of the fluctuation of N_b value for the polyhedron of the mobile cation. (d) The MTM power spectrum of the displacement $|r_i(t)|$ of the mobile central cation shown in (c). (See Appendix B for the details of the motions and structures of polyhedra.)

to the localized ion found at 400 K, which has a smaller fluctuation of N_b. Thus, the decrease in the floppy (zero frequency) mode is related to the stability of the polyhedron, and they are accompanied by the volume change at both T_B (or T_c) and T_g.

K. Comparison of ionics in the ionic liquid and ionically conducting glasses

For the network modifier in alkali silicate glasses such as Li ions in the case of lithium silicates, the loss of the geometrical degree of freedom of the LiO_x units does not mean the arrest of them, and further changes in the cages of Li ions are possible at temperatures below T_g. Therefore, ions have appreciable diffusivity (or conductivity) in the glassy networks formed by the SiO_4 units.

In the alkali silicate system, the glass transition temperature, T_g, and fragility of the system are affected by the contents of the alkali metal ions, M,[1] where the network of SiO_4 units are interrupted by the MO_x structures, which resulted in the softer structures of the system. The fragile character, represented by the non-Arrhenius behavior of the dynamics, increases with high alkali content,[24] and therefore, it is related to the mixing of different MO_x structures with distributions of N_V and N_b.

The situation of Li ions in lithium silicates with a distribution of coordination number is similar to the fragile ionic liquid, and it explains why the behavior of Li ion in the glass is compatible with that of ions in the super-cooled liquid, although several differences exist between them. One of the differences is considered as follows. In more fragile systems, the trapped species is also forming a cage of other particles, and therefore, it has a comparable mobility with the species surrounding it. This dual character will cause more complex ionic motion than Li in the silicate systems. That is, ionic motion in the silicate glass is decoupled from the silicate network, while the motions of cations and anions in the ionic liquid are coupled. More complicate polyhedral structures with the overlaps of the networks with larger N_V values are found in the ionic liquid than the case in the lithium silicate with smaller N_V values. In the former, the correlation between the motion of central ion and cages seems to be weaker.

L. Relation with thermodynamic scaling

Thus, from the results presented in the above, the glass transition in the present system is characterized by the rigidity and soft percolation of the bonds and cages. One of other
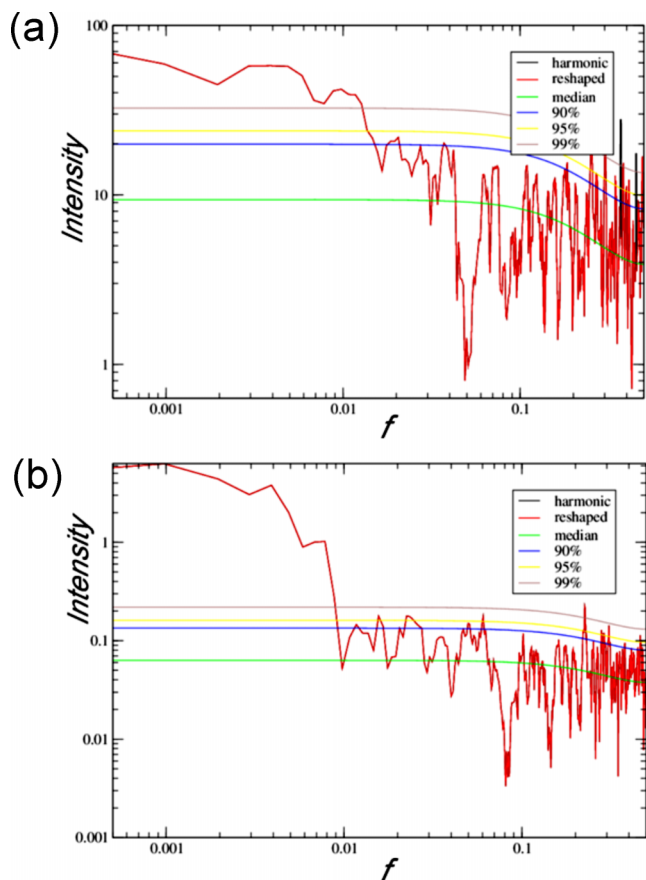
FIG. 15. (a) The MTM power spectrum of the fluctuation of N_b values of the polyhedron for the localized cation at 250 K. Relatively larger intensity of the spectrum at $f \sim 0$ is found for the fluctuation of N_b. (b) The MTM power spectrum for the displacement $|r_i(t)|$ of the cation. Existence of the power law region is not clearly observed and the zero frequency mode is negligibly small for the displacement. (See Appendix B for the details of the motions.).

atures and pressures ranges. Temperature and pressure dependences of the system are well described by the master function of the product variable, TV^{γ}, with $\gamma = 4.0$ and 3.8 for cation and anion, respectively. Temperature and pressure dependences of the pair correlation function show similar trend, and therefore can be super-positioned onto the master curve. Structures and Coulombic terms of the corresponding states on the master curve are found to be quite similar. The master curve of TV^{γ} shows an inflection at around T_B and the scaling seems to break down near the T_g.[62,63] Existence of the inflection point implies a change in the compressibility of the system, and this is naturally related to the packing of the polyhedra.

The thermodynamic scaling holds for many systems with different fragilities and nonexponentialities. Therefore, a viable theory of glass transition has to be sufficiently general in order to cover the same property of these diverse systems. From the existence of the thermodynamic scaling, pressure dependence of the system can be treated on an equal footing as temperature dependent behavior of the system. Validity of the thermodynamic scaling of dynamic properties in many glass forming liquids suggests that we should consider the packing of the coordination polyhedra in relation to the glass transition problem. This is because the dynamics having inflection points at temperatures T_B and T_g are associated with the corresponding changes in temperature dependence of volume.

M. Related works

There are several works using the concept of topological constraint on the problem of glass transition and the characteristics of glass. Here, we compared our results to some of them.

Topological constraint theory can explain many features of glasses, such as thermal, mechanical, and rheological properties of glasses.[68] Mauro[68] and Thorpe[10] also argued that the fraction of zero-frequency (i.e., floppy) modes is precisely zero at $\langle r \rangle \sim 2.4$, as floppy regions still exist after the rigid regions have percolated.

Recently, 2D binary soft-core system was examined by Aharanov *et al.*[16] The coordination numbers other than 6 are referred to as "defects" by using a time-honored Voronoi polygon construction. They define a typical scale $\xi \equiv 1/\sqrt{c_l}$, where c_l is a concentration of the liquid-like defects. It was considered to be related to the relaxation time. They predict that the relaxation time diverges where $c_l \to 0$, and it was regarded as the glass transition. Thus, effectively the decrease of the floppy mode resulted in the glass transition. If we assume the polyhedra with $N_b < (3N_V - 6)$ or $N_V = 4$ as defects, similar concept might be applicable also to ionic liquid, because the mode is almost smeared out at a certain temperature. In spite of the similarities, explanation given in our present work is different on several points. First, apparent divergence of the length scale related to this mode may occur at T_B or T_c rather than T_g. Second, the characteristics of defects in considering soft percolation of the connecting cages are more complicated, where the distributions of N_V and N_b are wider, and the mobility of the trapped particles is governed by both N_V and N_b and outer shells. Third, particle has a mobility even in the case with $N_b > (3N_V - 6)$ in the soft cages.

possible approaches for the glass transition is based on the observation of the property of thermodynamic scaling,[54–67] and this was previously examined for the same IL[63] and in the present work by MD simulation. In this section, the relation with this approach is discussed. Recently, thermodynamic scaling is found to be valid for many kinds of glass forming systems with different degrees of fragility; namely, τ_α or other transport coefficients obtained at various thermodynamic conditions can be scaled to become a unique function of the product variable, TV^{γ}, where γ is a material constant.[54–67] This thermodynamic scaling is commonly found for molecular and ionic systems including ionic liquids.[62,63] Such scaling holds rigorously if the underlying potential function is an inverse power law. Recently, we have presented evidences from experiments and simulation that the scaling behaviors started from the Johari-Goldstein β–relaxation or the primitive relaxation of the coupling model, which terminates the caged molecule (or ion) regime.[67] The existence of relation between the caged dynamics at short times and the development of diffusive dynamics at longer times suggests the relevance of the current study of the caged structures.

In the previous work,[63] MD simulations have been performed to study the scaling of dynamics near the glass transition regime of the ionic liquid, EMIM-NO$_3$, over wide temper-

N. Relation between slowing down of the dynamics and dynamical length scale

In this section, relation with a treatment of glass transition by considering the dynamical length scale and our results is discussed.

Often the divergence of some dynamical correlation length-scale on decreasing temperature (or decreasing volume) is assumed or expected for fragile glass-forming systems, although so far no direct evidence of divergence has been reported to the best of our knowledge. The structure shown by the breaking of the fictive bonds, or properties related to the multi-time correlation functions, has been used for such treatments.[3–6] Dynamical heterogeneity thus found is compatible with the mobile regions showing jump motions of particles.[7] Time scale of the dynamics (τ_α or related quantities) in the system is discussed with a correlation with dynamical length scale ξ obtained, as found in Ref. 3. The structure factor of the "broken" bonds $S_b(q)$ is

$$S_b(q) = \frac{1}{N_b} \left\langle | \sum_{\langle i,j \rangle} \exp(iq \cdot R_{ij})|^2 \right\rangle, \tag{6}$$

where N_b is a number of the "broken" bonds during $[t_0, t_0 + a\tau_b]$, where a is a constant.

By using the Ornstein-Zernike relation,

$$S_b(q) = S_b(0)/(1 + \xi^2 q^2), \tag{7}$$

the characteristic length scale ξ can be determined.

The time scale was connected to ξ by[3]

$$\tau_b \sim \xi^z. \tag{8}$$

Similar approach for the dynamical length scale can be found in Ref. 4. Although the Ornstein-Zernike relation fits well the data at the highest T, it fails at lower T, making the interpretation of the fitted ξ values ambiguous as discussed in Ref. 4. Increasing dynamical length scale is so far found for several systems but the length seems to be limited to the relatively small sizes. Recently, Pal and Biswas[6] have estimated the dynamic correlation length in an ionic liquid, 1-butyl-3-methylimidazolium-hexafluorophosphate (BMIM-PF$_6$) by analyzing a four point correlation function via the Ornstein-Zernike relation. The length scale thus found was ~9 Å at 298 K and 7 Å at 450 K. The length seems not large enough to account for the glass transition by itself, notwithstanding the fact that the system size effect exists.

Generally, a bond is broken when the jump motion of particle has occurred. When we consider diffusive motion, the time scale $\tau_\alpha \sim t_{\text{dif}}$ and the dynamical length scale during this time are not for single jump event but for accumulated and cooperative events of many particles. The dynamical length scale is a measure of such events spreading over in space, while the time scale is more directly governed by interval of jumps and correlations among jump events. The two are parallel consequences of the many-body relaxation and diffusion governed by the interaction terms of the potential, and connection between length-scale and time is possible, especially in the system with fractal characters.

The path of ions in the lithium silicates has been confirmed[69] to have larger dimension than 2.53, which is the value

of the percolation threshold in 3-dimensions,[70] and hence the percolation of the paths. Therefore, the formation of infinitive networks of mobile region does not mean the arrest of ions. In the lithium metasilicate melt and glass, fast translational motion of ions with cooperativity tends to show forward correlated jumps at longer time scale and is considered to be the main component of the diffusive motion.[71] Similar character of jumps is found by several authors,[72,73] although the details depend on the definition of fast and slow ions. Suppression of cooperative jumps in ionics in ionically conducting glasses is caused by decreasing temperature or by decreasing dimension of paths,[74] and it seems to be a general behavior of the jump diffusion.

V. CONCLUSION

We have considered the network structures formed by bonds and cages to address the glass transition problem in the fragile ionic liquid, EMIM-NO$_3$.

Conclusion is given here along with the three purposes mentioned in the Introduction. First, the existence of the changes of network properties at T_B and T_g is shown. With decrease in temperature, we have observed the increase of the shortest cation-anion (Coulombic) bonds resulting in the saturation of the degrees of the freedom of the system near T_g as well as increase in the number of connections of fictive bonds. Thus, the glass transition is similar to the rigidity percolation for these bonds. Second, we have characterized the cages, and the local structures in the network, and their changes on decreasing temperature by using the coordination number, N_V, and the number of bonds, N_b, within the coordination polyhedron. We introduced a concept of soft percolation of the cages with fictive bonds to characterize the earlier changes in the volume, partial potential energies, and dynamics near T_B higher than T_g, coming from the fragile behavior. Coordination polyhedra with fictive bonds play a role to determine the packing of the local structures. Soft percolation of cages can explain the dynamics of glass transition of the fragile systems showing changes of temperature dependence of the diffusion coefficient at two temperatures, T_B and T_g. Geometrical degrees of the freedom of the cages are saturated at T_B rather than T_g in the case of fragile system. That is, the structure with $N_V = 4$ and $N_b < (3N_V - 6)$ with other N_V values almost disappeared at T_B, where the system still have measurable diffusivity in MD simulations. Further change of the structure on cooling below T_B accompanied with changes in the distributions of N_v and N_b, and diffusive motion by jumps can continue until T_g is reached.

Third, Dynamic properties of trapped ion in the cage were characterized by using N_V and N_b, and its relation with the displacement of ions is discussed. The complexity of trajectories of ions determining the slowing down of dynamics, as well as the floppy mode in the power spectra, is related to the observed complexity of the structures of the system.

The complexity of the fragile system (soft character) considered here comes from the following sources.

1. Wide distribution of coordination number and fictive bonds;
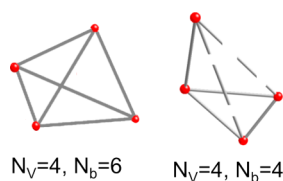2. multiple characters of networks, which is related to a dual character of trapped species and those forming cages;

$N_V=4, N_b=6$ $N_V=4, N_b=4$

FIG. 16. Concept of geometrical degree of freedom of the coordination polyhedron.[30] Trapped ions or atoms are not shown. Examples of the structure with $N_V = 4$. Here, N_V is a number of vertices, and N_b is number of fictive bonds (contact pairs). Broken bonds have lengths longer than the certain criterion (for example, we used the minimum position of $g(r)$ for the anion-anion pair). When $N_b = 3N_V - 6$, the freedom for the deformation of the polyhedron is lost. This concept is valid for silicate system so far examined.

3. multiple characters of networks related to the different kinds of bonds, attractive ones, and fictive ones with repulsive interactions.

The rigidity and/or softer percolation of bonds or cages can play a role in governing the dynamic of glass transition to various degrees of the systems with different fragility.

Networks of bonds or cages used to characterize the system are strongly correlated with the changes of volume, potential energies, and dynamics in the system. Further examination of the fragile ionic liquid and other systems including the lifetime of substructures is desirable for additional confirmation of mechanism proposed in this paper.
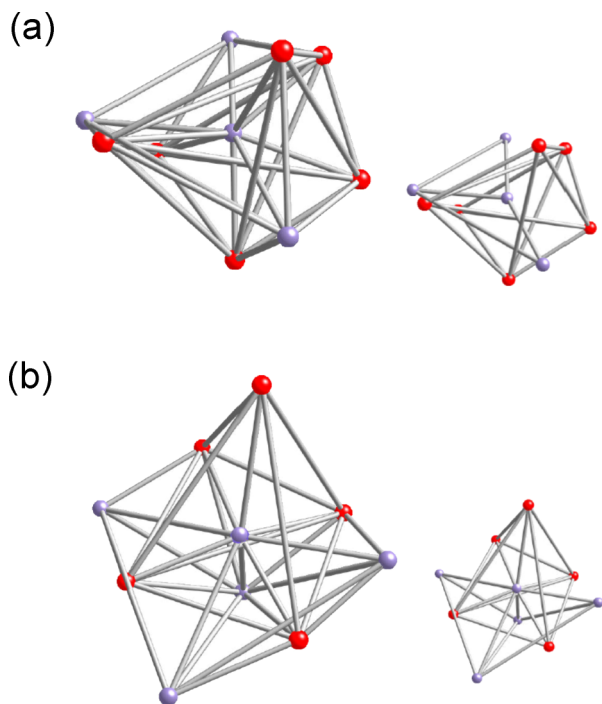

FIG. 17. (a) Instantaneous structure of a cluster for a localized central cation (see also Fig. 18(a)) taken at 400 K (~T_B). The ions within a $g(r)_{min}$ (7 Å) from the central cation (pale blue) are shown. Fictive bonds for the cation-cation pairs and anion-anion pairs within $g(r)_{min}$ are also shown. It contains a coordination polyhedron made of anions (red) around the cation ($N_V = 6$ and $N_b = 13$) and some neighboring cations within the distance. Thus, the network of polyhedra of cations around an anion and the opposite cases is deeply mixing. (b) Structure of a cluster for a mobile central cation within the distance of $g(r)_{min}$ (7 Å) from the central cation (see Fig. 18(b)). It consists of coordination polyhedra by anions ($N_V = 5$ and $N_b = 9$) and some cations as shown by the inset.
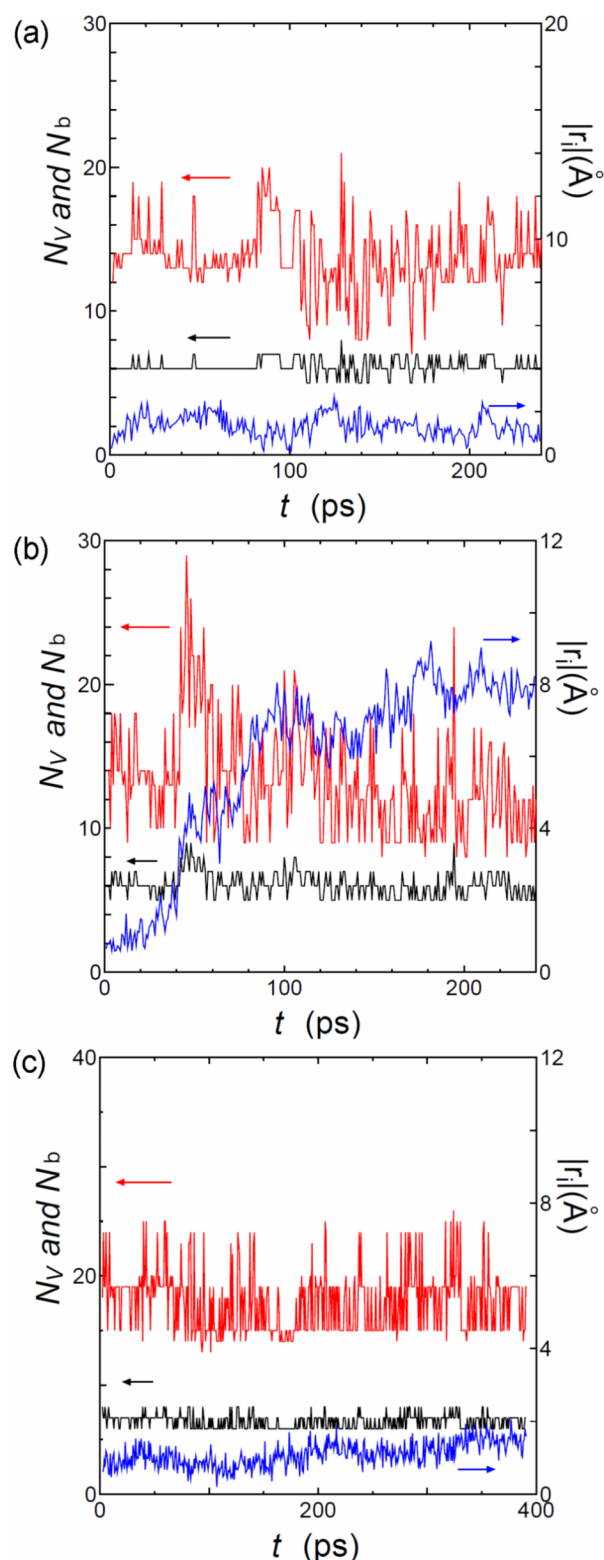

FIG. 18. (a) The motion of the central cation accompanied with the fluctuation of the N_V and N_b values of the polyhedron was examined by the center of the mass positions. Time dependence of N_V (black) and N_b (red) for an arbitrary chosen coordination polyhedron formed by NO_3^- ion around a localized $EMIM^+$ ion. The displacement $|r_i(t)|$ (blue, right axis) of the central ion was compared with the deformation of the polyhedron. (b) Similar plots for the mobile cation. The large displacement is accompanied with the changes of N_V and N_b values. Changes of both positive and negative directions of these values are related to the diffusive motion. Both examples are taken at 400 K. (c) Similar plots for an immobile cation at 250 K.

In other systems including other ionic liquids, factors such as "shapes" or "size ratio" of atoms or ions will affect the dynamics of the systems. It will be interesting to examine the validity of the concept of soft and rigidity percolation in these systems.

ACKNOWLEDGMENTS

APPENDIX A: CONCEPT OF GEOMETRICAL DEGREE OF FREEDOM OF THE COORDINATION POLYHEDRON

Concept of the geometrical degree of freedom is schematically shown in Fig. 16 for the case of $N_V = 4$. As shown in this example, to fix the shape of the polyhedra with $N_V = 4$, "$3N_V - 6$" fixed bonds are necessary. The "bond" in the present work can be fictive one (contact pair).

APPENDIX B: EXAMPLES OF POLYHEDRA AND THEIR FLUCTUATIONS

Two typical examples of polyhedra are taken near T_B. The clusters including these coordination polyhedra are shown in Fig. 17. (The structure is an instantaneous one.) Each figure contains a coordination polyhedron made of anions around a cation. Some neighboring cations within this distance are also shown to elucidate the mixing of different networks. The bonds connecting anions may be shared with other polyhedra and therefore are redundant. Even two bonds can cross and the maximum number of the bonds is given by $N_b = (1/2) N_V(N_V - 1)$ for all the combinations of pairs rather than by $N_b = (3N_V - 6)$. These structures in Figs. 17(a) and 17(b) show small and large displacements as in Figs. 18(a) and 18(b), respectively. For these cases, time dependent changes in $N_V(t)$ and $N_b(t)$ are also shown.

Time dependent change of N_V and N_b is well correlated with that of the central ion, although the changes of $|r_i(t)|$ are not necessarily in the same direction as the fluctuation of N_b or N_V. The displacement of an immobile cation at 250 K was examined in a similar manner and shown in Fig. 18(c).

[1] C. A. Angell, J. Non-Cryst. Solids **73**, 1 (1985).

[2] (a) J. Habasaki and K. L. Ngai, J. Chem. Phys. **129**, 194501 (2008); (b) Anal. Sci. **24**, 132 (2008).

[3] R. Yamamoto and A. Onuki, Phys. Rev. E **58**, 3515 (1998).

[4] C. Bennemann, C. Donati, J. Baschnagel, and S. C. Glotzer, Nature **399**, 248 (1999); C. Donati, S. C. Glotzer, and P. H. Poole, Phys. Rev. Lett. **82**, 5064 (1999).

[5] S. A. Reinsberg, A. Heuer, B. Doliwa, and H. W. Spiess, J. Non-Cryst. Solids **307-310**, 208 (2002).

[6] T. Pal and R. Biswas, J. Chem. Phys. **141**, 104501 (2014).

[7] R. Yamamoto and A. Onuki, Phys. Rev. Lett. **81**, 4915 (1998).

[8] J. C. Phillips, J. Non-Cryst. Solids **34**, 153 (1979); **43**, 37 (1982); Solid State Phys. **37**, 93 (1981); Rep. Prog. Phys. **59**, 1133 (1996).

[9] M. F. Thorpe, J. Non-Cryst. Solids **57**, 355 (1983).

[10] H. He and M. F. Thorpe, Phys. Rev. Lett. **54**, 2107 (1985).

[11] R. Böhmer and C. A. Angell, Phys. Rev. B **45**, 10091 (1992).

[12] W. Bresser, P. Boolchand, and P. Suranyi, Phys. Rev. Lett. **56**, 2493 (1986).

[13] P. Boolchand, R. N. Enzweiler, R. L. Cappellett, W. A. Kamitakahara, Y. Cai, and M. F. Thorpe, Solid State Ionics **39**, 81 (1990).

[14] M. Tatsumisago, B. L. Halfpap, J. L. Green, S. M. Lindsay, and C. A. Angell, Phys. Rev. Lett. **64**, 1549 (1990).

[15] W. A. Kamitakahara, R. L. Cappellett, P. Boolchand, B. L. Halfpap, F. Gompf, B. A. Neuman, and H. Mutka, Phys. Rev. B **44**, 94 (1991).

[16] E. Aharonov, E. Bouchbinder, H. G. E. Hentschel, V. Ilyin, N. Makedonska, I. Procaccia, and N. Schupper, Euro. Phys. Lett. **77**, 56002 (2007).

[17] S. Kohara, J. Akola, H. Morita, K. Suzuya, J. K. R. Weber, M. C. Wilding, and C. J. Benmore, Proc. Natl. Acad. Sci. U.S.A. **108**, 14785 (2011).

[18] D. J. Jacobs and M. F. Thorpe, Phys. Rev. E **53**, 3682 (1996).

[19] J. Habasaki, Mol. Phys. **70**, 513 (1990).

[20] J. Habasaki, I. Okada, and Y. Hiwatari, "Molecular dynamics simulations," Springer Ser. Solid-State Sci. **103**, 98 (1991).

[21] J. Habasaki, Z. Naturforsch. **46a**, 616 (1991).

[22] D. G. Georgiev, P. Boolchand, and M. Micoulaut, Phys. Rev. B **62**, R9228 (2000).

[23] K. L. Ngai and J. Habasaki, J. Chem. Phys. **141**, 114502 (2014), and references therein.

[24] Experimentally, fragility index, m, of silica, lithium trisilicate, lithium disilicate, lithium metasilicate is known to be 17.9, 26.3, 34.7 and 33.9, respectively., M. L. F. Nascimentoa and C. Aparicio, J. Phys. Chem. Solids **68**, 104 (2007).

[25] L. Jin, S. de Leeuw, M. V. Koudriachova, J. M. Pringle, P. C. Howlett, F. Chend, and M. Forsyth, Phys. Chem. Chem. Phys. **15**, 19570 (2013); J. B. Hooper and O. Borodin, ibid. **12**, 4635–4643 (2010); J. M. Pringle, P. C. Howlett, D. R. MacFarlane, and M. Forsyth, J. Mater. Chem. **20**, 2056–2062 (2010).

[26] R. Fabian, Jr. and D. L. Sidebottom, Phys. Rev. B **80**, 064201 (2009).

[27] D. J. Jacobs and M. F. Thorpe, Phys. Rev. E **53**, 3682 (1996).

[28] P. Boolchand, X. Feng, and W. J. Bresser, J. Non-Cryst. Solids **293-295**, 348 (2001).

[29] J. Habasaki and I. Okada, Mol. Sim. **9**, 319–326 (1992).

[30] A. L. Loeb, Space Structures (Addison-Wesley, 1976).

[31] K. L. Ngai, J. Habasaki, C. León, and A. Rivera, Z. Phys. Chem. **219**, 47–70 (2004).

[32] A. Pimenov, P. Lunkenheimer, H. Rall, R. Kohlhaas, A. Loidl, and R. Böhmer, Phys. Rev. E **54**, 676 (1996).

[33] P. Lunkenheimer, A. Pimenov, M. Dressel, Y. G. Goncharov, R. Böhmer, and A. Loidl, Phys. Rev. Lett. **77**, 318 (1996).

[34] X. Liu and H. Jain, J. Phys. Chem. Solids **55**, 1433 (1994).

[35] K. L. Ngai, J. Chem. Phys. **110**, 10576 (1999); K. L. Ngai and C. León, Phys. Rev. B **66**, 064308 (2002).

[36] J. Habasaki, K. L. Ngai, and Y. Hiwatari, Phys. Rev. E **66**, 021205 (2002); J. Chem. Phys. **120**, 8195–8200 (2004); K. L. Ngai, J. Habasaki, Y. Hiwatari, and C. León, J. Phys.: Condens. Matter **15**, S1607–1632 (2003).

[37] J. Wang, R. M. Wolf, J. W. Caldwell, P. A. Kallamn, and D. A. Case, J. Comput. Chem. **25**, 1157 (2004).

[38] D. A. Case, V. Babin, J. T. Berryman, R. M. Betz, Q. Cai, D. S. Cerutti, T. E. Cheatham III, T. A. Darden, R. E. Duke, H. Gohlke, A. W. Goetz, S. Gusarov, N. Homeyer, P. Janowski, J. Kaus, I. Kolossváry, A. Kovalenko, T. S. Lee, S. LeGrand, T. Luchko, R. Luo, B. Madej, K. M. Merz, F. Paesani, D. R. Roe, A. Roitberg, C. Sagui, R. Salomon-Ferrer, G. Seabra, C. L. Simmerling, W. Smith, J. Swails, R. C. Walker, J. Wang, R. M. Wolf, X. Wu, and P. A. Kollman, AMBER 14 (University of California, San Francisco, 2014).

[39] K. L. Ngai, Relaxation and Diffusion in Complex Systems (Springer, New York, 2011).

[40] J. Habasaki and K. L. Ngai, J. Non-Cryst. Solids **357**, 446 (2011).

[41] T. C. Halsey, M. H. Jensen, L. P. Kandanoff, I. Procaccia, and B. I. Shraimn, Phys. Rev. A **33**, 1141 (1986), With coexistence of different length scales, the density profile formed has a multifractal character.

[42] J. Habasaki and A. Ueda, J. Chem. Phys. **134**, 084505 (2011); **138**, 144503 (2013).

[43] W. Xu, E. I. Cooper, and C. A. Angell, J. Phys. Chem. B **107**, 6170 (2003).

[44] N. D. Khupse and A. Kumar, J. Solution Chem. **38**, 589 (2009).

[45] M. G. del Popolo and G. A. Voth, J. Phys. Chem. B **108**, 1744 (2004).

[46] T. Yan, C. J. Burnham, M. G. del Popolo, and G. A. Voth, J. Phys. Chem. B **108**, 11877 (2004).

[47] B. Mandelbrot, Science **155**, 636 (1967).

[48] H. Cang, J. Li, and M. D. Fayer, J. Chem. Phys. **119**, 13017 (2003).

[49] R. A. Pethrick, F. M. Jacobsen, O. E. Morgensen, and M. Eldrup, J. Chem. Soc., Faraday Trans. 2 **76**, 225 (1980).

[50] K. L. Ngai, L.-R. Bao, A. F. Yee, and C. L. Soles, Phys. Rev. Lett. **87**, 215901 (2001).

[51]N. C. Forero-Martinez, R. Cortes-Huerto, and P. Ballone, J. Chem. Phys. **136**, 204510 (2012).

[52]G. Dlubek, Y. Yu, R. Krause-Rehberg, W. Beichel, S. Bulut, N. Pogodina, I. Krossing, and Ch. Friedrich, J. Chem. Phys. **133**, 124502 (2010).

[53]M. Ghil, R. M. Allen, M. D. Dettinger, K. Ide, D. Kondrashov, M. E. Mann, A. Robertson, A. Saunders, Y. Tian, F. Varadi, and P. Yiou, Rev. Geophys. **40**(1), 3.1-3.41 (2002).

[54]A. Tölle, H. Schober, J. Wuttke, O. G. Randl, and F. Fujara, Phys. Rev. Lett. **80**, 2374 (1998).

[55]L. Berthier and G. Tarjus, Phys. Rev. Lett. **103**, 170601 (2009).

[56]H. C. L-Higgins and B. Widom, Mol. Phys. **8**, 549 (1964); A. Tölle, Rep. Prog. Phys. **64**, 1473 (2001).

[57]C. Dreyfus, A. Aouadi, J. Gapinski, M. M-Lopes, W. Steffen, A. Patkowski, and R. M. Pick, Phys. Rev. E **68**, 011204 (2003).

[58]C. A-Simionesco, D.D. Kivelson, and G. Tarjus, J. Chem. Phys. **116**, 5033 (2002).

[59]R. L. Cook, H. E. King, C. A. Herbst, and D. R. Herschbach, J. Chem. Phys. **100**, 5178 (1994).

[60]S. Sastry, PhysChemComm **3**, 79 (2000).

[61]S. Mossa, E. La Nave, H. E. Stanley, C. Donati, F. Sciortino, and P. Tartaglia, Phys. Rev. E **65**, 041205 (2002).

[62]R. R. Casalini and C. M. Roland, Phys. Rev. E **69**, 062501 (2004); C. M. Roland, S. Bair, and R. Casalini, J. Chem. Phys. **125**, 124508 (2006).

[63]J. Habasaki, R. Casalini, and K. L. Ngai, J. Phys. Chem. B **114**, 3902 (2010).

[64]E. R. López, A. S. Pensado, M. J. P. Comuñas, A. A. H. Pádua, J. Fernández, and K. R. Harris, J. Chem. Phys. **134**, 144507 (2011).

[65]A. S. Pensado, A. A. H. Pádua, M. J. P. Comuñas, and J. Fernández, J. Phys. Chem. B **112**, 5563 (2008).

[66]M. Paluch, S. Haracz, A. Grzybowski, M. Mierzwa, J. Pionteck, A. Rivera-Calzada, and C. León, J. Phys. Chem. Lett. **1**, 987 (2010).

[67]K. L. Ngai, J. Habasaki, D. Prevosto, S. Capaccioli, and M. Paluch, J. Chem. Phys. **137**, 034511 (2012); **140**, 019901 (2014).

[68]J. C. Mauro, Am. Ceram. Soc., Bull. **90**(4), 31 (2011).

[69]J. Habasaki and K. L. Ngai, J. Chem. Phys. **122**, 214725 (2005).

[70]N. Jan and D. Stauffer, Int. J. Mod. Phys. C **9**, 341 (1998).

[71]J. Habasaki, I. Okada, and Y. Hiwatari, Phys. Rev. B **55**, 6309 (1997).

[72]A. Heuer, M. Kunow, M. Vogel, and R. D. Banhatti, Phys. Chem. Chem. Phys. **4**, 3185 (2002); M. Vogel, Phys. Rev. B **68**, 184301 (2003).

[73]R. A. Montani, C. Balbuena, and M. A. Flechero, Solid State Ionics **209-210**, 5 (2012).

[74]J. Habasaki and K. L. Ngai, Phys. Chem. Chem. Phys. **9**, 4673 (2007).